THE DELIGNE COMPLEX FOR THE B_3 ARTIN GROUP

KATHERINE GOLDMAN, AMY HERRON

ABSTRACT. We show that the piecewise Euclidean Moussong metric on the Deligne complex of the Artin group of type B_3 is CAT(0). We do this by establishing a criteria for a complex made of B_3 simplices to be CAT(1) in terms of embedded edge paths, which in particular applies to the spherical Deligne complex of type B_3. This provides one more step to showing that the Moussong metric is CAT(0) for any 3-dimensional Artin group.

CONTENTS

1. INTRODUCTION

Artin groups are closely tied to Coxeter groups. While Coxeter groups are largely well-understood, there are still a plethora of open questions regarding the Artin groups. One of the most prominent of these is the $K(\pi, 1)$ conjecture, which essentially asks if a specific space is an Eilenberg-MacLane space for a given Artin group. This turns out to be equivalent to asking if an object called the "(modified) Deligne complex" is contractible [CD95]. One common technique in geometric group theory and metric geometry for showing spaces are contractible is to show that they possess some notion of non-positive curvature. Recent success has been had using various new ideas of non-positive curvature [PS21, Hae23, Hua24]. But it has long been conjectured that Deligne complexes are CAT(0) under a specific metric, typically called the Moussong metric, defined in terms of the Davis complex of the associated Coxeter group [CD95, Conj. 3]. Very few Artin groups are known to satisfy this; in fact, it is only known when the group is 2-dimensional [CD95, Thm. 4] or if the only "spherical-type" subdiagrams of its Coxeter-Dynkin diagram are either edges or A_3 [Cha04].

It is notoriously difficult to show that piecewise spherical cell complexes of dimension ≥ 2 are CAT(1). Broadly, this is because it requires establishing that any loop of length $< 2\pi$ is not a (local) geodesic. In [EM02], a method is presented for showing arbitrary 2-dimensional piecewise spherical simplicial complexes are CAT(1), via excluding certain "galleries". Although an explicit list of galleries is given, it is quite large, and generally unfeasible to apply to Artin groups directly. In [Cha04], this is overcome by cleverly using the geometry of A_3 simplices and the relationship of the Deligne complex with the Coxeter complex to reduce the study of all galleries to just a few which stay in the 1-skeleton. This is the inspiration for our current work.

Our method for simplifying the study of general loops to edge paths is made somewhat more simple by using a slightly altered criteria developed by Bowditch for a locally CAT(1) space to be CAT(1). This criteria says that in order for a locally CAT(1) space to be CAT(1), all short loops must be "shrinkable" to the trivial loop. Since shrinkability is an equivalence relation, we are able to easily reduce to the edge paths by showing that an arbitrary short loop is shrinkable to a short closed edge path.

While we perform a similar reduction to edge paths as in the A_3 case, there are a number of other paths that now must be ruled out. To show that the spherical Deligne complex for the braid group on four strands is CAT(1), Charney needed to essentially consider two configurations of geodesic edge paths; one of edge length 4, and one of edge length 6. For the spherical Deligne complex of type B_3, one must consider paths of edge length 4, 6, 8, and 10. The geometry of the spherical Deligne complex of type B_3 also becomes much less friendly than type A_3, which requires the implementation of new tools to analyze these edge paths. We are able to confirm that all edge paths are shrinkable, and therefore, we add B_3 to the collection of Artin groups with CAT(0) Deligne complex:

Theorem 5.12. *The (piecewise spherical) Moussong metric on the spherical Deligne complex of type B_3 is* CAT(1).

The most general setting in which this may be applied is the following.

Theorem 5.13. *Suppose $A(\Gamma)$ is a 3-dimensional Artin group and Γ contains no subdiagram of type H_3. Then the (piecewise Euclidean) Moussong metric on the Deligne complex for $A(\Gamma)$ is* CAT(0) *and, in particular, $A(\Gamma)$ satisfies the $K(\pi, 1)$ conjecture.*

Example 1.1. Some new examples of diagrams Γ which give Artin groups $A(\Gamma)$ whose Deligne complexes are now known to have a CAT(0) Moussong metric can be seen in Figure 1.

It turns out, in fact, that our method for showing this spherical Deligne complex is CAT(1) may also be applied to a more general class of 2-dimensional simplicial complexes. For clarity, and for broader application, we have extracted the necessary criteria thusly. The full definitions are given in Section 2.

Theorem 2.1. *Suppose X is a B_3 simplicial complex satisfying each of the following conditions:*

(1) *The link of every vertex is nonempty and connected.*
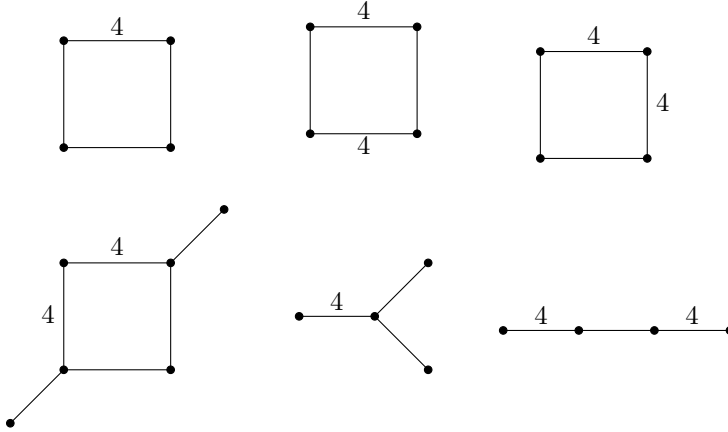(2) *If v is a vertex of type $\hat{s}_1$, then $lk(v, X)$ has girth at least 8.*

FIGURE 1. New Coxeter-Dynkin diagrams

(3) *If v is a vertex of type $\hat{s}_2$, then $lk(v, X)$ is complete bipartite, partitioned along types of vertices, and contains at least one embedded 4-cycle.*
(4) *If v is a vertex of type $\hat{s}_3$, then $lk(v, X)$ has girth at least 6.*
(5) *Any path in the 1-skeleton of X which passes through vertices of the type seen in Figure 2 is contained in a subcomplex of X of the corresponding type in Figure 3.*
(6) *The 10-cycles of the form in Figure 4 are not embedded.*

Then the B_3 metric on X is CAT(1).

Following this, in Section 3, we will discuss the necessary background and general definitions surrounding Coxeter and Artin groups, along with some of their respective complexes. Section 4 includes more specific properties of these complexes in the case of type B_n that will be needed later in the paper, notably including a novel proof that the Artin group of type B_n embeds into type A_{2n-1} in a certain well-behaved way. The majority of this section is devoted to this new proof, which is done using mapping class groups. Section 5 uses new techniques to show certain paths are shrinkable, implying the spherical Deligne complex of type B_3 satisfies the hypotheses of Theorem 2.1, completing the proof that the metric is CAT(1).

2. A COMBINATORIAL CRITERIA FOR CAT(1) B_3 COMPLEXES

Let Δ denote a spherical 2-simplex on vertex set $\{\hat{s}_1, \hat{s}_2, \hat{s}_3\}$, where the internal angle at $\hat{s}_1$ is $\pi/4$, the angle at $\hat{s}_2$ is $\pi/2$, and the angle at $\hat{s}_3$ is $\pi/3$. We will call a pure 2-dimensional simplicial complex X a B_3 *(simplicial) complex* if for every 2-simplex σ of X, there is an isomorphism $m_\sigma : \sigma \to \Delta$, and if for every vertex v

and 2-simplices σ and τ containing v, we have $m_\sigma(v) = m_\tau(v)$. (In other words, the 1-skeleton of X has a coloring by $\{\hat{s}_1, \hat{s}_2, \hat{s}_3\}$.) If v is a vertex of a 2-simplex σ, we will call $m_\sigma(v)$ the *type* of the vertex v. There is a canonical metric on X obtained by pulling back the metric of Δ along the maps m_σ, which we call the B_3 metric on X. Our main theorem is the following.

Theorem 2.1. *Suppose X is a B_3 simplicial complex satisfying each of the following conditions:*

(1) *The link of every vertex is nonempty and connected.*
(2) *If v is a vertex of type $\hat{s}_1$, then $lk(v, X)$ has girth at least 8.*
(3) *If v is a vertex of type $\hat{s}_2$, then $lk(v, X)$ is complete bipartite, partitioned along types of vertices, and contains at least one embedded 4-cycle.*
(4) *If v is a vertex of type $\hat{s}_3$, then $lk(v, X)$ has girth at least 6.*
(5) *Any path in the 1-skeleton of X which passes through vertices of the type seen in Figure 2 is contained in a subcomplex of X of the corresponding type in Figure 3.*
(6) *The 10-cycles of the form in Figure 4 are not embedded.*

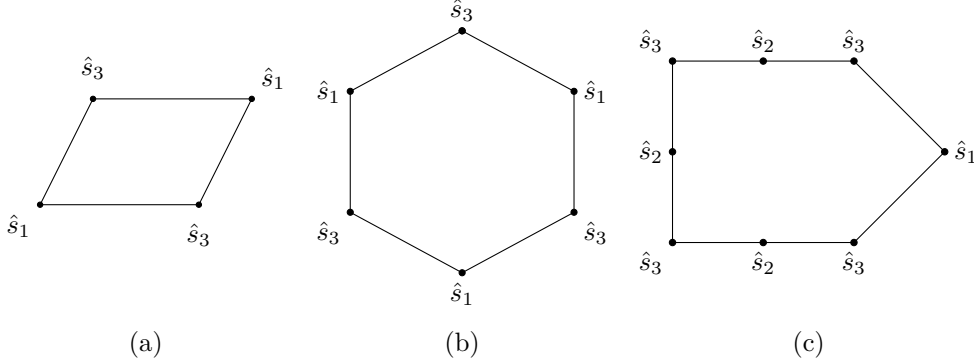*Then the B_3 metric on X is* CAT(1).

FIGURE 2. Some short closed edge paths

In order to show that these complexes are CAT(1), we utilize the following criteria of Bowditch [Bow95, §3]

Proposition 2.2. *If X is locally* CAT(1), *then X is* CAT(1) *if and only if every rectifiable loop of length $< 2\pi$ is "shrinkable".*

We will call a rectifiable path *short* if it has length $< 2\pi$. A loop is a closed path. We say that rectifiable loops α and β are 2π-*homotopic* (or *short homotopic*) and write $\alpha \sim_s \beta$ if there is a (free) homotopy from α to β through short loops (i.e., each loop in the homotopy is a short rectifiable loop). If $\gamma \sim_s 0$ (where 0 is any constant loop), we say that γ is *shrinkable*.

The conditions (2), (3), and (4) guarantee that the B_3 metric on X is locally CAT(1), so we only need to show that short loops are shrinkable. In order to show that there are no unshrinkable short loops in X, we first show that an arbitrary short loop is short homotopic to a loop remaining in the 1-skeleton of X (an "edge
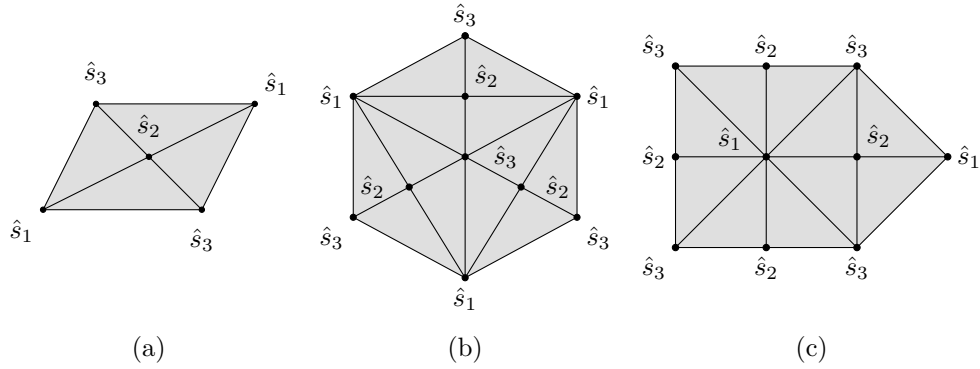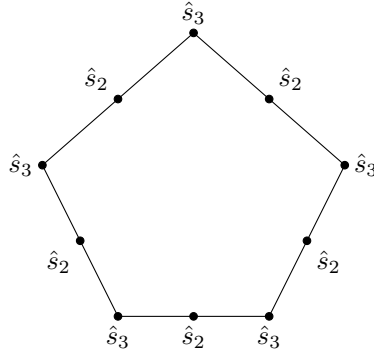
FIGURE 3. Filled edge paths

FIGURE 4. A non-admissible loop

loop"), then show that all short edge loops are short homotopic to one of the loops in Figure 2 or Figure 4. Then conditions (5) and (6) guarantee these loops are shrinkable.

For the rest of Section 2, we assume X is a B_3 simplicial complex endowed with its B_3 metric, satisfying the hypotheses of Theorem 2.1.

Before continuing, we provide a quick observation.

Lemma 2.3. *X is a flag complex.*

Proof. Let $\{v_1, v_2, v_3\}$ be a set of vertices of X which are pairwise adjacent, with e_{ij} the edge between v_i and v_j. Since X is a pure 2-dimensional complex, each e_{ij} is contained in a 2-simplex σ_{ij}. By considering the maps $m_{\sigma_{ij}}$, each of v_1, v_2, and v_3 must have distinct types. Without loss of generality, suppose v_i has type $\hat{s}_i$ for each i. Then since $lk(v_2, X)$ is complete bipartite, there is an edge between the points in the link representing v_1 and v_3; this edge represents the fact that $\{v_1, v_2, v_3\}$ spans a simplex.

Suppose $\{v_1, v_2, v_3, \ldots v_n\}$ is a set of pairwise adjacent vertices. By similar reasoning to above, each of these vertices must have distinct labels. However, there are only 3 labels, so we cannot have $n > 3$. $\square$

2.1. **Shrinking to edge loops.** We now perform the reduction from arbitrary short loops to loops which stay in the 1-skeleton.

The proof of the following lemma is identical to the proof of [Gol25, Lemma 5.5] given by the first author.

Lemma 2.4. *Suppose $v_1, v_2 \in X$ are distinct vertices of type $\hat{s}_2$. Then $St(v_1) \cap St(v_2)$ is either empty, a single vertex, or a single (closed) edge.*

Let $C(B_3)$ denote the unit 2-sphere with its standard tessellation by copies of the B_3 simplex Δ, along with the vertex labeling induced by Δ. Important to the forthcoming proofs is the notion of *developing* a geodesic from X to $C(B_3)$ [Cha04]. The notion of developing in the context of locally CAT(1) spaces originated in [EM02]. Charney was able to simplify this method by developing these geodesics onto the spherical Coxeter complex rather than an arbitrary 2-sphere.

Suppose γ is a local geodesic of X which does not intersect any vertices. Then the sequence of 2-simplices which intersect γ can be mapped one-by-one to a sequence of adjacent (and distinct) 2-simplices of $C(B_3)$ such that the vertex labeling is preserved. Since adjacency is preserved, these maps may be glued to form a locally injective map from a subcomplex of X onto a subcomplex of $C(B_3)$. The image of γ under this map is a local geodesic $\overline{\gamma}$ in $C(B_3)$, called the *development of γ (onto $C(B_3)$)*.
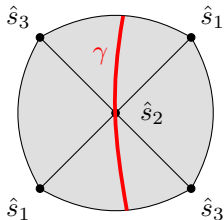

FIGURE 5. Developing a geodesic through a vertex of type $\hat{s}_2$

We may also develop local geodesics which intersect vertices of type $\hat{s}_2$ in the following way. If γ is a local geodesic which passes through a vertex v of type $\hat{s}_2$, then it intersects the ε-sphere of v at two points which are distance at least π apart in the round/unit/link metric on the ε-sphere. By its definition, this sphere is isometric to the link of v, so the points on the sphere correspond to points in the link which are distance no less than π apart. Since the link is complete bipartite and the lengths of edges are $\pi/2$, the diameter of the link is precisely π, so these points are exactly distance π apart. Moreover, these points are contained in a loop of edge length 4, corresponding to four 2-simplices of X which form a quadrilateral as in Figure 5. These simplices can then be mapped down to $C(B_3)$, and the image $\overline{\gamma}$ of γ will still be locally geodesic at the image of v. Because we can develop over a vertex of type $\hat{s}_2$ but not $\hat{s}_1$ or $\hat{s}_3$ in general, we will call vertices of type $\hat{s}_2$ *nonsingular* and vertices of type $\hat{s}_1$ and $\hat{s}_3$ *singular*.

Lemma 2.5. *If γ is a nontrivial short closed local geodesic which intersects no singular vertices, then $\ell(\gamma) \geq \pi$.*
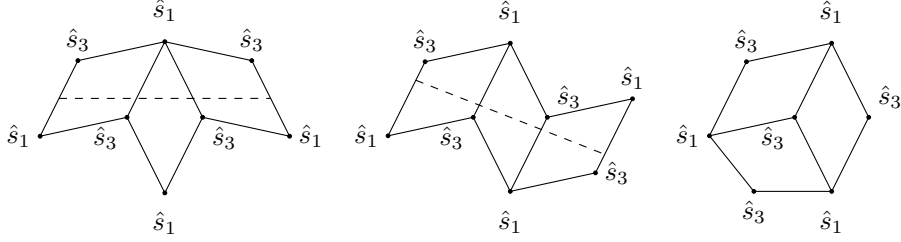
FIGURE 6. Quadrilateral galleries of length three

Proof. If $\ell(\gamma) < \pi$, then there are no more than 3 (not necessarily distinct) vertices v_1, v_2, v_3 of type $\hat{s}_2$ such that $\gamma \cap st(v_i) \neq \varnothing$. (Otherwise if γ intersects 4 or more stars of distinct $\hat{s}_2$-type vertices, then by developing, we see that $\ell(\gamma) > \pi$.) We know $|\{v_1, v_2, v_3\}| \neq 1$, since this would contradict the fact that X is simplicial, and we know $|\{v_1, v_2, v_3\}| \neq 2$ since this would contradict Lemma 2.4. Thus each vertex v_1, v_2, and v_3 are distinct. By developing, this gives one of the three galleries of quadrilaterals in Figure 6. In this figure, the dashed lines are examples of geodesics, and one should think of these quadrilaterals as "filled" as in Figure 2(a), where the central vertices are the images of v_1, v_2, and v_3.

In $C(B_3)$, the development $\overline{\gamma}$ is a local (hence global) geodesic of length $< \pi$, so cannot be closed since $C(B_3)$ is CAT(1). Thus $\overline{\gamma}$ is a geodesic segment in one of these galleries with endpoints on the boundary, and the edges/vertices containing these endpoints are identified in X. If any edges or vertices in the left-most or right-most diagrams are identified in X, this would contradict Lemma 2.4, so γ cannot develop onto galleries of these forms.

Consider the middle gallery. None of the vertices of the middle quadrilateral of this gallery can be identified with any other vertices in the gallery, so the only possible identifications are left-most vertices (or edge) with right-most vertices (resp., edge) of the diagram. But in each case, this induces a loop of length 4 of the type in Figure 2(a) which can be filled by a vertex v_4 of type $\hat{s}_2$, by condition (5). If $v_4 = v_i$ for some $i = 1, 2, 3$, then this contradicts Lemma 2.4, since some pair v_i and v_j ($i, j = 1, 2, 3$ distinct) would have $St(v_i) \cap St(v_j)$ either the union of an edge and a (disjoint) vertex, or the union of two (distinct) edges. If $v_4 \neq v_i$ for each $i = 1, 2, 3$, then this again contradicts Lemma 2.4: $St(v_4)$ will intersect one of the $St(v_i)$ ($i = 1, 2, 3$) in two distinct edges, depending on the labeling of the quadrilaterals. Regardless, we know γ cannot develop onto a gallery of this shape, and thus $\ell(\gamma) \geq \pi$. $\qquad\square$

Lemma 2.6. *Suppose γ is a short closed local geodesic. Then there is a short closed loop $\gamma' \sim_s \gamma$ such that γ' intersects a singular vertex of X.*

Proof. Of course, if γ already intersects a singular vertex, there is nothing to show. So, assume γ intersects no singular vertices of X. By Lemma 2.5, we know $\ell(\gamma) \geq \pi$, so let a and b be two values such that $d(\gamma(a), \gamma(b)) = \pi$. Develop γ to a local geodesic $\overline{\gamma}$ in $C(B_3)$. Then $\overline{\gamma}(a)$ and $\overline{\gamma}(b)$ are antipodal points of the unit sphere $C(B_3)$. There is a natural homotopy of the segment $\overline{\gamma}|_{[a,b]}$ in $C(B_3)$ obtained by rotating relative to its endpoints until the segment intersects a singular vertex of

$C(B_3)$. Each curve in the homotopy (until the final curve) contains no singular vertices in its interior, and thus can be lifted back to X to obtain a homotopy of $\gamma|_{[a,b]}$ relative to its endpoints through segments of length π to a segment which contains a vertex. (The final curve can be added by taking a pointwise limit of this homotopy.) By concatenating this homotopy with the rest of γ, we obtain a short homotopy from γ to a loop containing a vertex. $\square$
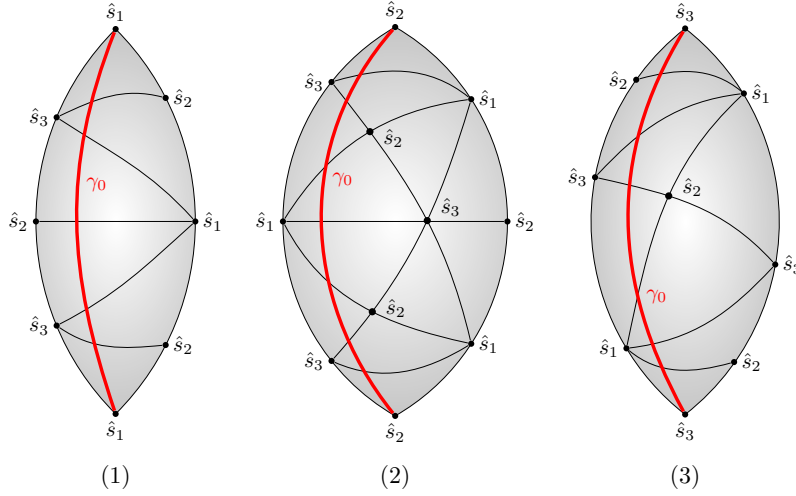

FIGURE 7. The lunes with terminal vertices of type $\hat{s}_1$, $\hat{s}_2$, and $\hat{s}_3$, resp.

Lemma 2.7. *Suppose γ is a short closed local geodesic which intersects a singular vertex. Then there is a short closed edge path γ' with $\gamma' \sim_s \gamma$.*

Proof. Decompose γ into a concatenation $\gamma_0 \gamma_1 \ldots \gamma_n$ of geodesic segments which contain no singular vertices in their interior. Notice that for each i, this means either γ_i is an edge path or contains no edges in its interior. Suppose γ_i contains no edges. We can develop γ_i onto $C(B_3)$, resulting in one of the diagrams (1) or (3) of Figure 7. (The development can pass through the vertex of type $\hat{s}_2$ with no issues.) The endpoints of this development are at distance π from each other, so we may rotate the development to lay on the boundary of its respective lune, and lift this rotation to get a length-preserving homotopy of γ_i to an edge path. $\square$

The following lemma holds in much greater generality than our current setting, so we provide this more general proof here for reference.

Proposition 2.8. *Suppose Y is a locally $\mathrm{CAT}(1)$ piecewise spherical simplicial complex with $\mathrm{Shapes}(Y)$ finite. Let γ be a short loop based at $x_0 \in Y$. Then either $\gamma \sim_s 0$, or there exists a closed local geodesic γ' based at x_0 such that $\gamma \sim_s \gamma'$.*

Proof. Let $\Omega = \Omega(Y, x_0, 2\pi)$ denote the space of loops in Y based at x_0 with length $< 2\pi$, equipped with the supremum metric $d_\Omega(\alpha, \beta) = \sup d_X(\alpha(t), \beta(t))$. Note that the length function $\ell : \Omega \to [0, \infty)$ is lower semi-continuous with respect to

this metric. Let Ω' denote the connected component of Ω containing γ, and let $I = \inf \ell(\Omega')$. Choose a sequence $\{\gamma_n\}$ in Ω' such that $\lim \ell(\gamma_n) \to I$.

Since Y is locally CAT(1) and Shapes(Y) is finite, Y is actually "uniformly locally CAT(1)", meaning that for sufficiently small ε, given any point $y \in Y$, the ε-neighborhood about x is CAT(1). (This follows quickly from Theorem I.7.39 and Lemma I.7.56 from [BH13].) This implies we can shrink the elements of the sequence $\{\gamma_n\}$ to piecewise geodesic with a uniformly bounded number of geodesic subsegments. In more detail: fix n, and let $U_{n,0}$ denote the ε neighborhood about $x_{n,0} := x_0$. Choose a point $x_{n,1}$ which is distance $> \varepsilon/2$ from x_0 and in the same connected component of $U_{n,0} \cap \gamma_n$ as x_0. Let $U_{n,1}$ denote the ε ball around $x_{n,1}$. Continuing in this fashion, we have a finite set of points $\{x_{n,0}, \ldots, x_{n,k_n}\}$ on γ_n and ε-balls $\{U_{n,0}, \ldots, U_{n,k_n}\}$ covering γ_n, with $U_{n,i}$ centered at $x_{n,i}$. But since the lengths of the γ_n are uniformly bounded, the sequence $\{k_n\}$ must be bounded as well, say $k_n \leq M$. For any n, if $i > k_n$, define $x_{n,i} = x_0$ and $U_{n,i} = U_{n,0}$. Notice that by our definition, the segment of γ_n between $x_{n,i}$ and $x_{n,i+1}$ is contained in $U_{n,i}$, which is CAT(1). Hence this segment can be shrunken to the (unique) geodesic segment between $x_{n,i}$ and $x_{n,i+1}$. Doing this for each i yields a piecewise geodesic loop $\overline{\gamma}_n$ which is short homotopic to γ_n. Note also that the number of points at which the γ_n are not geodesic (which we will call the *break points*) is uniformly bounded. By abuse of notation, we replace γ_n with this piecewise geodesic $\overline{\gamma}_n$.

Now since γ_n is piecewise geodesic, it is contained in a finite subcomplex $K_n \subseteq Y$. Because the number of break points of the γ_n are uniformly bounded and Shapes(Y) is finite, there is a uniform bound on the number of cells in the K_n. Then since Shapes(Y) is finite, this implies there is a subsequence $\{\gamma_{n_i}\}$ such that K_{n_i} is isometrically isomorphic to K_{n_j} for all i and j, via some map $\varphi_{ij} : K_{n_i} \to K_{n_j}$. For each i and j, let $\gamma_{ij} = \varphi_{ij}(\gamma_{n_i})$, and for $k = 0, \ldots, M$, let $x_{ij}^{(k)} = \varphi_{ij}(x_{i,k})$, so that $\{x_{ij}^{(0)}, \ldots, x_{ij}^{(M)}\}$ forms the set of break points of γ_{ij}. Then for $n \geq 0$ and $k = 0, \ldots, M$, the sequence $\{x_{in}^{(k)}\}_{i=1}^{\infty}$ has a convergent subsequence (it is contained in the compact space K_j). In particular, we can find a common subsequence $\{x_{i_j n}^{(k)}\}_{j=1}^{\infty}$ which converges for each $k = 0, \ldots, M$. Let $x_n^{(k)} = \lim_{j \to \infty} x_{i_j n}^{(k)}$ for each $k = 0, \ldots, M$, and let $\hat{\gamma}_n$ be the concatenation of the (unique) geodesic segments from $x_n^{(k)}$ to $x_n^{(k+1)}$.

Choose N large enough so that $d_X(x_{i_j N}^{(k)}, x_N^{(k)}) < \varepsilon/2$ for all $j \geq N$ and all $k = 0, \ldots, M$. Let $K = K_N$ and consider the sequence $\{\gamma_{i_j N}\}_{j=N}^{\infty}$. Then, for all $j \geq N$ and each $k = 0, \ldots, M$, since $d_X(x_{i_j N}^{(k)}, x_{i_j N}^{(k+1)}) < \varepsilon/2$ (by our original definition of the piecewise geodesics γ_n), and $d_X(x_{i_j N}^{(k)}, x_N^{(k)}) < \varepsilon/2$, it follows that $d_X(x_{i_j N}^{(k+1)}, x_N^{(k)}) < \varepsilon$. Note that we also have $d_X(x_N^{(k)}, x_N^{(k+1)}) < \varepsilon/2$. In summary, the points $x_{i_j n}^{(k)}, x_{i_j N}^{(k+1)}$, and $x_N^{(k+1)}$ are contained in the ε-ball centered at $x_N^{(k)}$. In particular, this ball also contains the geodesics between respective pairs of these points. Since each such ball is CAT(1), the convergence of the break points of the $\gamma_{i_j N}$ implies uniform convergence of the sequence $\{\gamma_{i_j N}\}$ to $\hat{\gamma}_N$ in X (i.e., convergence in the sup metric). Then since the length function is lower semicontinuous,

$$I = \liminf \ell(\gamma_{i_j N}) \geq \ell(\lim \gamma_{i_j N}) = \ell(\hat{\gamma}_N) \geq I,$$

so $\ell(\hat{\gamma}_N) = I = \inf \ell(\Omega_0)$. But in addition, again since this ε-ball is CAT(1), the homotopy from $x_{i_j N}^{(k)}$ to $x_N^{(k)}$ along the geodesic segment between them, and the homotopy from $x_{i_j N}^{(k+1)}$ to $x_N^{(k+1)}$ along the geodesic segment between them, together induce a short (free) homotopy from the (unique) geodesic segment between $x_{i_j N}^{(k)}$ and $x_{i_j N}^{(k+1)}$ to the (unique) geodesic segment between $x_N^{(k)}$ and $x_N^{(k+1)}$. In other words, for $j \geq N$, $\gamma_{i_j N} \sim_s \hat{\gamma}_N$. This means $\hat{\gamma}_N \sim_s \gamma$.

If $I = 0$, then we must have that $\hat{\gamma}_N$ is a constant loop, so $\gamma \sim_s 0$. Suppose then that γ is not shrinkable, i.e., that $I > 0$. Assume also that $\hat{\gamma}_N$ is not locally geodesic. Then there are points p, q on $\hat{\gamma}_N$ so that one of the segments of $\hat{\gamma}_N$ between p and q is not a geodesic. Replacing this segment with the unique geodesic between p and q would give a loop in Ω_0 which has strictly shorter length than $\hat{\gamma}_N$, contradicting the fact that $\ell(\hat{\gamma}_N) = \inf \ell(\Omega_0)$. Thus $\hat{\gamma}_N$ is locally geodesic. $\square$

Theorem 2.9. *If γ is a short loop, then there is a short closed edge path γ' with $\gamma \sim \gamma'$.*
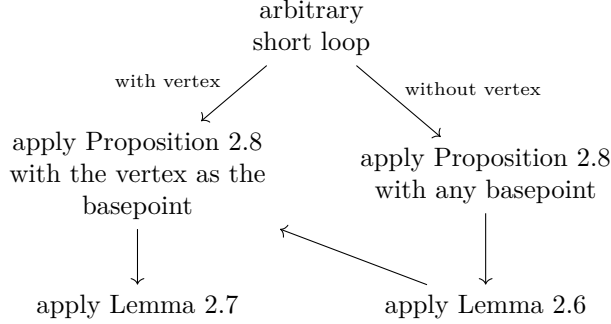

FIGURE 8. A flow chart for the proof of Theorem 2.9

Proof. If $\gamma \sim_s 0$, there is nothing to show, so suppose γ is not shrinkable. Suppose then that γ intersects some singular vertex v of X. Then we may apply Proposition 2.8 with basepoint v to obtain a short closed local geodesic γ_1 based at v with $\gamma \sim_s \gamma_1$. By Lemma 2.7, there is an edge path γ' with $\gamma' \sim_s \gamma_1$, and so $\gamma \sim_s \gamma'$.

Now suppose γ does not intersect a singular vertex of X. Then apply Proposition 2.8 (with any basepoint) to obtain a short closed local geodesic γ_1 with $\gamma_1 \sim_s \gamma$. Lemma 2.6 gives a short loop γ_2 with $\gamma_1 \sim_s \gamma_2$ such that γ_2 intersects some singular vertex $v \in D(B_3)$. Applying Proposition 2.8 again, this time based at v, gives a short closed geodesic γ_3 based at v with $\gamma_3 \sim_s \gamma_2$. We can then apply Lemma 2.7 to get an edge path γ' with $\gamma' \sim_s \gamma_3$, and in particular, $\gamma' \sim_s \gamma$. $\square$

2.2. **Further edge path reduction.** Next, we work to reduce arbitrary short closed edge paths to the list in Figure 2.

Let s_i denote the edge of Δ opposite $\hat{s}_i$ for $i = 1, 2, 3$. Then let α be the length of s_1, β the length of s_2, and δ the length of s_3. Then

$$\alpha = \arccos\left(\frac{\sqrt{2}}{\sqrt{3}}\right) \approx 0.615$$

$$\beta = \arccos\left(\frac{1}{\sqrt{3}}\right) \approx 0.955$$

$$\delta = \arccos\left(\frac{1}{\sqrt{2}}\right) \approx 0.785.$$

The maps m_σ give rise an edge labeling of X. We will call an edge e *type s_i* whenever $m_\sigma(e)$ is the edge s_i in Δ.

We can rule out certain combinations of edges as possible loops immediately. For example, since X is a flag complex, any loop of edge length 3 must be filled by a simplex and thus is shrinkable. Similarly, X is simplicial, so it contains no digons and every edge is embedded. Hence we may restrict ourselves to loops of edge length ≥ 4. We may also restrict our consideration to embedded edge paths; if a path is not embedded, we may reparameterize it to be a union of embedded closed edge paths which we may shrink separately. Thus in the following, all closed edge paths are assumed to be embedded unless stated otherwise.

For the following further reduction, for $i = 1$ or 3, say that a segment in the 1-skeleton of X is "type $2s_i$" if it is the union of a pair of (distinct) edges of type s_i which meet at a vertex of type $\hat{s}_2$.

Lemma 2.10. *Any closed edge path of X can be shrunken to a closed edge path consisting only of (distinct) segments of type $2s_i$ for $i = 1, 3$, and an even number of edges of type s_2.*

Proof. Let γ be an edge path. Suppose there are adjacent edges e_1 and e_3 in γ of type s_1 and s_3, respectively. These edges meet at a vertex v in γ of type $\hat{s}_2$, and give rise to a vertex of type $\hat{s}_3$ and $\hat{s}_1$, resp., in the link of v. Since the link of a type $\hat{s}_2$ vertex is complete bipartite, there is an edge in the link connecting these vertices, which corresponds to a 2-simplex containing e_1 and e_3. Let e_2 be the other edge of this 2-simplex, necessarily of type s_2. Then γ can be shrunken by replacing the concatenation of e_1 and e_3 with e_2. In other words, we may assume that for any closed edge path, the two edges adjacent to an edge of type s_1 must be type s_1 and type s_2, and similarly the two edges adjacent to an edge of type s_3 must be type s_3 and type s_2. Since there are no digons, this implies such a path contains only edges of type $2s_1$, s_2, and $2s_3$.

Note that the endpoints of a segment of type $2s_1$ are vertices of type $\hat{s}_3$, and the endpoints of a segment of type $2s_3$ are vertices of type $\hat{s}_1$. But the segments of type s_2 have exactly one endpoint which is a vertex of type $\hat{s}_1$ and exactly one endpoint which is a vertex of type $\hat{s}_3$. Since $\hat{s}_i$ vertices cannot be adjacent to $\hat{s}_i$ vertices (for $i = 1, 2, 3$), this means each possible edge loop must have an even number of edges of type s_2. $\square$

In particular, this means every closed edge path is shrinkable to a closed edge path with an even number of edges, so we may restrict our attention to such paths. With these restrictions, we list the remaining possible edge paths.

Suppose γ has $2n_\alpha$ edges of type s_1, $2n_\beta$ edges of type s_2, and $2n_\delta$ edges of type s_3. Then $\ell(\gamma) < 2\pi$ if and only if $2n_\alpha\alpha + 2n_\beta\beta + 2n_\delta\delta < 2\pi$. The triples $(n_\alpha, n_\beta, n_\delta)$ of non-negative integers which provide solutions to the latter inequality are shown in Table 1.

$(i, 0, 0)$, $i = 2, 3, 4, 5$	$(0, i, 0)$, $i = 2, 3$	$(0, 0, i)$, $i = 2, 3$
$(0, 1, i)$, $i = 1, 2$	$(0, 2, i)$, $i = 1$	$(1, 0, i)$, $i = 1, 2, 3$
$(1, 1, i)$, $i = 0, 1$	$(1, 2, 0)$,	$(2, 0, i)$, $i = 1, 2$
$(2, 1, i)$, $i = 0, 1$	$(3, 0, 1)$,	$(3, 1, 0)$

TABLE 1. $(n_\alpha, n_\beta, n_\delta)$ satisfying $2n_\alpha\alpha + 2n_\beta\beta + 2n_\delta\delta < 2\pi$

A segment of type $2s_1$ cannot be adjacent to a segment of type $2s_3$ (and vice versa), so the triples $(i, 0, j)$ for any $i > 0$ and $j > 0$ cannot correspond to an embedded loop. By Lemma 2.4, there are no embedded loops consisting of exactly two segments of type $2s_1$ or two segments of type $2s_3$. This shortens the list to the triples in Table 2.

$(i, 0, 0)$, $i = 3, 4, 5$	$(0, i, 0)$, $i = 2, 3$	$(0, 0, 3)$,
$(0, 1, i)$, $i = 1, 2$	$(0, 2, i)$, $i = 1$	$(1, 1, i)$, $i = 0, 1$
$(1, 2, 0)$,	$(2, 1, i)$, $i = 0, 1$	$(3, 1, 0)$

TABLE 2. A reduced list of triples $(n_\alpha, n_\beta, n_\delta)$

We can now show how certain cycles may be shrunken to those in Figure 2. First, the 4-cycles. The only short embedded 4-cycles which do not appear in Figure 2 are those appearing in Figure 9.
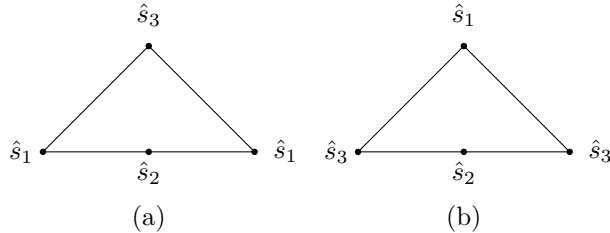

FIGURE 9. Remaining 4-cycles

Lemma 2.11. *Loops of the type in Figure 9 are contained in subcomplexes of the form in Figure 10.*
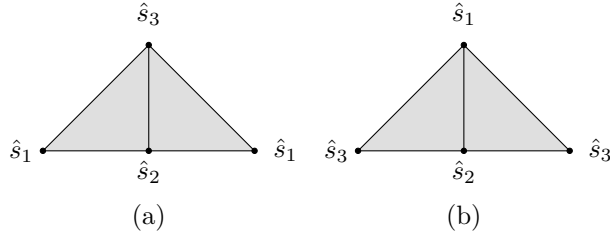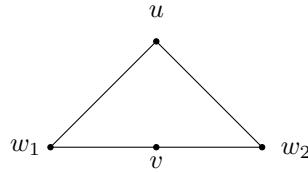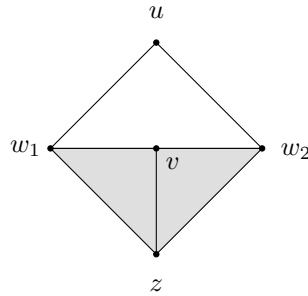
FIGURE 10. Filling the 4-cycles

Proof. Suppose γ is a(n embedded) loop of type (a). (The type (b) case is identical, switching the labeling of $\hat{s}_1$ and $\hat{s}_3$.) Let v denote the vertex of type $\hat{s}_2$, u the vertex of type $\hat{s}_2$, and w_1, w_2 the distinct vertices of type $\hat{s}_1$.

Since $lk(v)$ is complete bipartite, we can find a vertex z of type $\hat{s}_3$ adjacent to v, w_1, and w_2:

Now the induced cycle on the vertices u, w_1, z, and w_2 is an edge path of the type in Figure 2(a), thus can be filled by a vertex v' of type $\hat{s}_2$. If $v \neq v'$, this would contradict Lemma 2.4. Thus γ can be completed to

□
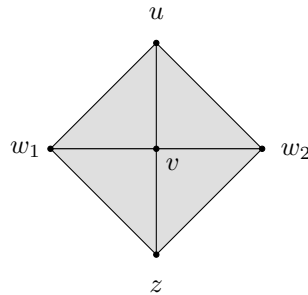
Lemma 2.12. *Every short embedded closed edge path in $D(B_3)$ of edge-length 6 is short-homotopic to an embedded closed edge path of the type in Figure 2(b).*

Proof. Let δ denote a segment which is the union of two adjacent edges of X meeting at a vertex v of type $\hat{s}_2$, such that the remaining two vertices w_1 and w_2 are both type $\hat{s}_1$ or both type $\hat{s}_3$. Then there is a vertex v' in the link of v which is adjacent to both w_1 and w_2 and has the opposite type (that being type $\hat{s}_3$ or $\hat{s}_1$, respectively). Let δ' denote the edge path between the vertices w_1, v', and w_2. This results in δ and δ' bounding a subcomplex of X of the form in Figure 10(b) or Figure 10(c). In either case, it is clear that δ is homotopic to δ' through a homotopy which is monotone in the lengths of its paths. In other words, we may replace an "$\hat{s}_1$-$\hat{s}_2$-$\hat{s}_1$" (or, an "$\hat{s}_3$-$\hat{s}_2$-$\hat{s}_3$") segment with an "$\hat{s}_1$-$\hat{s}_3$-$\hat{s}_1$" (resp., an "$\hat{s}_3$-$\hat{s}_1$-$\hat{s}_3$") segment in a "monotone" fashion.

As a consequence of this, if γ is a short edge loop containing a subpath δ as above, then γ is short homotopic to the path γ' obtained by replacing δ with δ' in γ. Any 6-cycle γ in Table 2 which is not the 6-cycle in Figure 2 contains a subpath δ of this form. After repeating this procedure on each such subpath, we see that γ is short homotopic to a 6-cycle of the form in Figure 2. $\square$

The only edge paths of length 8 that don't appear in Figure 2 are those of the type seen in Figure 11.
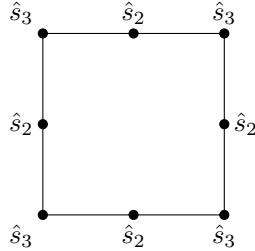

FIGURE 11. The other 8-cycle

The proof of the following Lemma is identical to the proof of Lemma 2.12.

Lemma 2.13. *An embedded 8-cycle of the form in Figure 11 is short-homotopic to an embedded 8-cycle of the form in Figure 2.*

Finally, the only short 10-cycle is the one appearing in Figure 4. However, we have assumed that such a cycle is never embedded. Thus we can complete the proof of Theorem 2.1.

Proof (of Theorem 2.1). Let γ_1 be an arbitrary embedded short loop. Using Theorem 2.9, we can find an embedded short edge loop γ_2 such that $\gamma_1 \sim_s \gamma_2$. Then using Lemmas 2.11, 2.12, and 2.13, we can find an embedded short loop γ_3 of the form in Figure 2 with $\gamma_2 \sim_s \gamma_3$. Condition (5) guarantees that $\gamma_3 \sim_s 0$, therefore $\gamma_1 \sim_s 0$. $\square$

3. BACKGROUND ON ARTIN GROUPS AND COXETER GROUPS

We can now focus on the main application of this result: the Deligne complex of an Artin group of type B_3. In this section, we introduce the notation that will be used throughout the rest of the paper.

A *Coxeter-Dynkin diagram* is a finite simplicial graph Γ equipped with a labeling $m : E(\Gamma) \to \mathbb{Z}_{\geq 3} \cup \{\infty\}$ of edges. Since Γ is simplicial, every edge $e \in E(\Gamma)$ can be written as an unordered pair of vertices $\{s, t\}$, and sometimes we write $m(s,t) = m(t,s) = m(\{s,t\}) = m(e)$. If $\{s,t\} \notin E(\Gamma)$, define $m(s,t) = m(t,s) = 2$. When illustrating a Coxeter-Dynkin diagram, it is common to omit labels on edges e with $m(e) = 3$.

Such a diagram defines a Coxeter group

$$W(\Gamma) = \langle\, s \in V(\Gamma) \mid (st)^{m(s,t)} = 1 \text{ if } m(s,t) \neq \infty, s^2 = 1 \,\rangle$$

and an Artin group

$$A(\Gamma) = \langle\, s \in V(\Gamma) \mid \underbrace{sts\ldots}_{m(s,t) \text{ letters}} = \underbrace{tst\ldots}_{m(s,t) \text{ letters}} \quad \text{if } m(s,t) \neq \infty \,\rangle.$$

We call a Coxeter-Dynkin diagram Γ *spherical* and an Artin group $A(\Gamma)$ *spherical-type* if $W(\Gamma)$ is finite.

We will write $\Lambda \leq \Gamma$ to denote a full subgraph Λ of Γ (i.e., if two vertices $x, y \in V(\Lambda)$ are adjacent in Γ, then they are also adjacent in Λ) which inherits the edge labeling of Γ. Then $A(\Lambda)$ is an Artin group which is isomorphic to the subgroup of Γ generated by $V(\Lambda)$ by sending the generators of $A(\Lambda)$ to the generators coming from the same vertex viewed inside Γ [vdL83]. By abuse of notation, we will identify these two groups. A similar statement holds for the Coxeter groups $W(\Lambda)$ and $W(\Gamma)$. A particular type of full subgraphs are the *maximal* full subgraphs. If $s \in V(\Gamma)$, then we let $\hat{s}$ denote the full subgraph of Γ on vertex set $V(\Gamma) \setminus s$. By abusing notation, we sometimes let $\hat{s} = A(\hat{s})$ or $\hat{s} = W(\hat{s})$; the meaning will be obvious by context.

For any Coxeter-Dynkin diagram Γ, we may associate a number of relevant cell complexes, two of which are the *Deligne complex* and the *Davis-Moussong complex*. Let $G = A(\Gamma)$ or $W(\Gamma)$. We define

$$\mathcal{S}^f = \{\, \Lambda \leq \Gamma : \Lambda \text{ is spherical} \,\}, and$$
$$G\mathcal{S}^f = \{\, gA(\Lambda) : g \in G, \Lambda \in \mathcal{S}^f \,\},$$

both partially ordered by standard inclusion. Since $G\mathcal{S}^f$ is a poset, we can form its derived poset $(G\mathcal{S}^f)'$, the set of linearly ordered subsets (or *chains*) of $G\mathcal{S}^f$, itself ordered by inclusion. Then $(G\mathcal{S}^f)'$ is an abstract simplicial complex, so we may form its geometric realization $|(G\mathcal{S}^f)'|$. When $G = W(\Gamma)$, we call this the *Davis-Moussong complex* $\Sigma(\Gamma)$, and when $G = A(\Gamma)$, we call this the *Deligne complex* $\Phi(\Gamma)$. (Note that in some literature, $\Phi(\Gamma)$ is called the *modified Deligne complex*.) In either case, G acts on $|(G\mathcal{S}^f)'|$ with strict fundamental domain isomorphic to $|(\mathcal{S}^f)'|$. A discussion of various natural metrics on $\Phi(\Gamma)$ and $\Sigma(\Gamma)$ are discussed in [CD95]. We will be interested in the *Moussong metric*, which we will not define explicitly here for reasons that will become evident. (The full definition can be found in [CD95, §4.4].)

The next of the complexes are the *Artin complex* and the *Coxeter complex*. Again, let G denote either $A(\Gamma)$ or $W(\Gamma)$, and define a simplicial complex $\Delta = \Delta(\Gamma)$

as follows. The vertex set of Δ is

$$\{ g\hat{s} : g \in G, s \text{ a vertex of } \Gamma \},$$

which is the collection of cosets of maximal standard parabolic subgroups of G. Note that every vertex v has a well-defined "type", that is, a *unique* vertex $s \in V(\Gamma)$ such that $v = g\hat{s}$; when this equality holds, we will say that v is *type* $\hat{s}$. A collection $\{g_0\hat{s}_1, \ldots, g_n\hat{s}_n\}$ of vertices span an n-simplex of Δ if and only if

$$\bigcap g_i\hat{s}_i \neq \varnothing.$$

When $G = A(\Gamma)$, we call Δ the *Artin complex* and denote it by $D(\Gamma)$. (Note that in some literature, $D(\Gamma)$ is called the *spherical Deligne complex*, or simply the *Deligne complex*. However, we reserve the latter name for our $\Phi(\Gamma)$.) When $G = W(\Gamma)$, we call Δ the *Coxeter complex* and denote it by $C(\Gamma)$.

The group G (for $G = A(\Gamma)$ or $W(\Gamma)$) acts naturally on Δ by left multiplication. This action has a strict fundamental domain of a $(|V(\Gamma)|-1)$-simplex with exactly one vertex of each type. If Γ is spherical, then $C(\Gamma)$ has a metric which makes it isometric to a standard round sphere in $\mathbb{R}^{|V(\Gamma)|-1}$ (hence the terminology "spherical" Coxeter-Dynkin diagram). Since the fundamental domains of the actions on $D(\Gamma)$ and $C(\Gamma)$ are isomorphic, when Γ is spherical we may endow $D(\Gamma)$ with a metric under which this isomorphism of fundamental domains becomes an isometry. By slight abuse of notation, we will call this metric on $D(\Gamma)$ the *(spherical) Moussong metric*. The key relationship between these various notions of Moussong metric is the following.

Proposition 3.1. [CD95] *The Moussong metric on $\Phi(\Gamma)$ is* CAT(0) *if and only if for every connected $\Lambda \in \mathcal{S}_\Gamma^f$, the spherical Moussong metric on $D(\Lambda)$ is* CAT(1).

If Γ is a diagram with the property that every $\Lambda \in \mathcal{S}_\Gamma^f$ has $|V(\Lambda)| \leq n$, then we call each of Γ, W_Γ, and A_Γ *n-dimensional*. (In this case, the Deligne complex and Davis-Moussong complex are n-dimensional simplicial complexes.)

4. GEOMETRY OF $D(B_n)$

To fix notation, we let A_n denote the Coxeter-Dynkin diagram

$$\underset{t_1}{\bullet}\rule{1cm}{0.4pt}\underset{t_2}{\bullet}\rule{1cm}{0.4pt}\underset{t_3}{\bullet} \cdots \underset{t_n}{\bullet}$$

and let B_n denote the Coxeter-Dynkin diagram

$$\underset{s_1}{\bullet}\rule{1cm}{0.4pt}\underset{s_2}{\bullet} \cdots \overset{4}{\underset{s_{n-1}}{\bullet}\rule{1cm}{0.4pt}\underset{s_n}{\bullet}}$$

We define a partial order on the vertices of $D(A_n)$ and $D(B_n)$ as follows. Let $u = s$ or t. For cosets $g_1\hat{u}_{i_1}$ and $g_2\hat{u}_{i_2}$, we say $g_1\hat{u}_{i_1} \leq g_2\hat{u}_{i_2}$ if $g_1\hat{u}_{i_1} \cap g_2\hat{u}_{i_2} \neq \varnothing$ and $i_1 \leq i_2$. To either vertex set we may formally adjoin a minimal element 0 satisfying $0 < g\hat{u}_i$ for all g and all i; we will denote the resulting poset by $D_0(A_n)$ and $D_0(B_n)$, respectively. One of the key technical lemmas we need is the following.

Proposition 4.1. [Hae23, Prop. 6.6] *The poset $D_0(B_n)$ is a graded semi-lattice of rank n with minimum 0, such that any pairwise upper bounded subset of $D_0(B_n)$ has a join.*

Within the proof of this Proposition, three important maps are defined, the first of which is the morphism $\phi : A(B_n) \to A(A_{2n-1})$ given by

$$s_i \mapsto t_i t_{2n-i} \text{ for } i \leq n-1,$$
$$s_n \mapsto t_n.$$

The second important map defined within the proof of Proposition 4.1 is the extension of ϕ to the Deligne complexes $\psi : D(B_n) \to D(A_{2n-1})$ by defining $\psi(g\hat{s}_i) = \phi(g)\hat{t}_i$ on the vertices. (This also induces a map $D_0(B_n) \to D_0(B_n)$ by sending 0 to 0.) This map is well-defined and preserves the ordering on the respective Deligne complexes.

The final map that we need that is defined within the proof of Proposition 4.1 is the involution $\sigma : A(A_{2n-1}) \to A(A_{2n-1})$ by $t_i \mapsto t_{2n-i}$. Then σ extends to an order-reversing involution on $D(A_{2n-1})$ by $\sigma(g\hat{t}_i) = \sigma(g)\hat{t}_{2n-i}$. Notice that for $g \in A(B_n)$, $\sigma(\psi(g\hat{s}_i)) = \phi(g)\hat{t}_{2n-i}$.

Haettel notes that ϕ is injective. Previous proofs of this use normal forms and Garside theory to initially show that ϕ restricted to positive monoids is injective. (See, for example, [Cri97].) We provide a novel proof using mapping class groups. The authors thank Dan Margalit for the idea and Johanna Mangahas for helping with the technical details.

Proposition 4.2. *The map $\phi : A(B_n) \to A(A_{2n-1})$ is a an injective homomorphism.*

We break up this proof into the following parts:

1. Define convenient homeomorphisms representing the generators of $\mathrm{Mod}(\mathbb{D}_{1,n})$ and $\mathrm{Mod}(\mathbb{D}_{1,2n})$,
2. Prove that $\Phi : \mathrm{Mod}(\mathbb{D}_{1,n}) \to \mathrm{Mod}(\mathbb{D}_{2n})$ is a homomorphism,
3. Prove that $\Phi : \mathrm{Mod}(\mathbb{D}_{1,n}) \to \mathrm{Mod}(\mathbb{D}_{2n})$ is injective,
4. Define the *mixed braid group* and recall some standard facts about the relationship between Artin groups, braid groups, and mapping class groups,
5. Define a series of maps that connect $\phi : A(B_n) \to A(A_{2n-1})$ to $\Phi : \mathrm{Mod}(\mathbb{D}_{1,n}) \to \mathrm{Mod}(\mathbb{D}_{2n})$, and
6. Complete the proof that $\phi : A(B_n) \to A(A_{2n-1})$ is injective.

Part 1:

We begin by defining mapping classes that will be used to prove that $\Phi : \mathrm{Mod}(\mathbb{D}_{1,n}) \to \mathrm{Mod}(\mathbb{D}_{2n})$ is a homomorphism. Define $\mathbb{D}_{2n,1}$ to be the closed disk with $2n$ punctures and one marked point in the middle as shown in the figure for part 1.a. Define $\mathbb{D}_{1,n}$ to be the closed disk with n punctures and one marked point at the end as shown in the figure for part 2.a. We will define specific mapping classes in $\mathbb{D}_{1,2n}$ and $\mathbb{D}_{1,n}$ and a quotient map that takes the defined mapping classes in $\mathbb{D}_{1,2n}$ to those in $\mathbb{D}_{1,n}$.

1. For $1 \leq i \leq n-1$

   a. Define $\tilde{f}_i : \mathbb{D}_{1,2n} \to \mathbb{D}_{1,2n}$ to be the two half Dehn twists shown below where $\times$ denotes the marked point and the punctures are numbered.
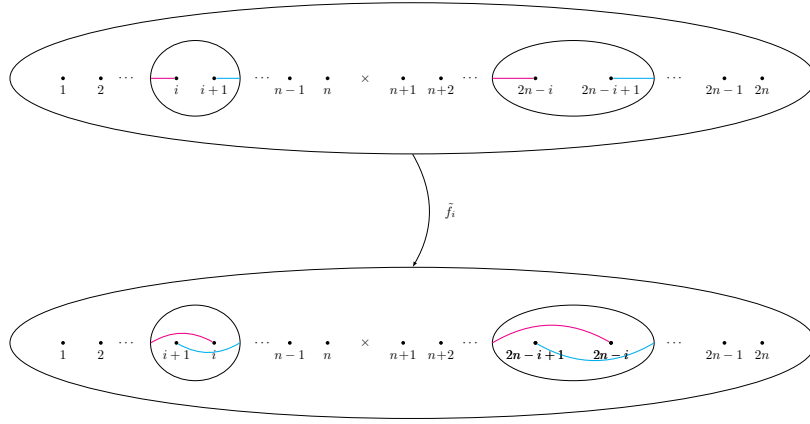
b. Define $f_i : \mathbb{D}_{1,n} \to \mathbb{D}_{1,n}$ to be the half Dehn twist shown below where $\times$ denotes the marked point and the punctures are numbered.
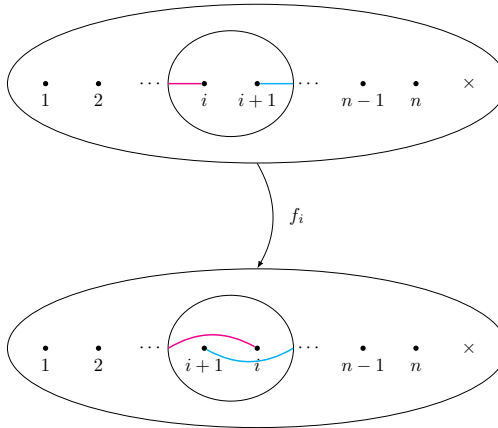
c. Next we justify our notation by defining a double branched cover $q_\times : \mathbb{D}_{1,2n} \to \mathbb{D}_{1,n}$. Consider $\mathbb{D}_{n+1}$ and $\mathbb{D}_{2n+1}$ as $\mathbb{D}_{1,n}$ and $\mathbb{D}_{1,2n}$ punctured at their marked points, respectively. Define $q : \mathbb{D}_{2n+1} \to \mathbb{D}_{n+1}$ as the double cover obtained by quotienting $\mathbb{D}_{2n+1}$ by a 180-degree rotation about the central puncture—formerly the marked point. Now we define $q_\times$ as follows: $q_\times = q$ on $\mathbb{D}_{2n+1} \subseteq \mathbb{D}_{1,2n}$; and $q_\times$ takes the marked point of $\mathbb{D}_{1,2n}$ to the marked point of $\mathbb{D}_{1,n}$. Thus, we see that $f_i q_\times = q_\times \tilde{f}_i$, which makes $\tilde{f}_i$ a lift of f_i.

2. For $i = n$ in $\mathbb{D}_{1,2n}$.

a. Define $\tilde{f}_n : \mathbb{D}_{1,2n} \to \mathbb{D}_{1,2n}$ to be the (full) Dehn twist about the annulus shown below. Observe that $\tilde{f}_n$ is a representative of the mapping class corresponding to the half Dehn twist swapping punctures n and $n+1$.
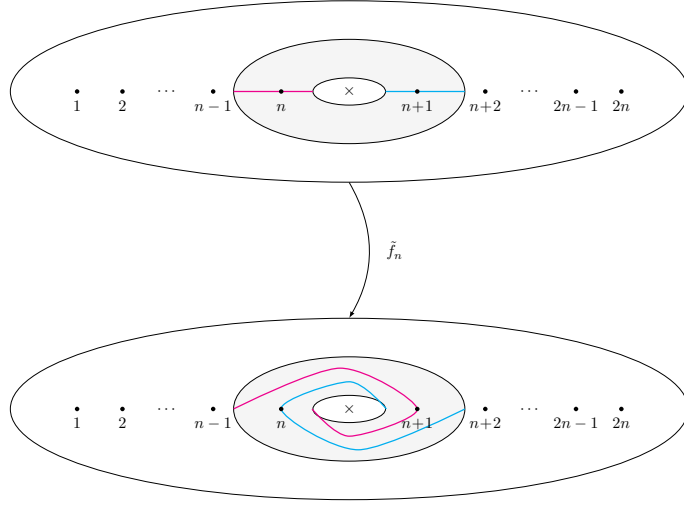
b. Note that map $\tilde{f}_n$ commutes with the 180-degree rotation used in defining q_x. Therefore there exists $f_n : \mathbb{D}_{1,n} \to \mathbb{D}_{1,n}$ such that $f_n q_x = q_x \tilde{f}_n$. Therefore $\tilde{f}_n$ is a lift of f_n.

3. Define Φ on generators such that $\Phi([f_i]) = forget([\tilde{f}_i])$, where $[g]$ is the mapping class of g and the *forget* map forgets the marked point in $\mathrm{Mod}(\mathbb{D}_{1,2n})$.

<u>Part 2</u>:

We are now ready to prove that map Φ is a homomorphism.

Proposition 4.3. *Map $\Phi : Mod(\mathbb{D}_{n,1}) \to Mod(\mathbb{D}_{2n})$ is a homomorphism.*

Proof. It suffices to show that if a product of generators $\prod[f_{\sigma(i)}]$ is the identity in $\mathrm{Mod}(\mathbb{D}_{1,n})$, then $\Phi(\prod[f_{\sigma(i)}])$ is the identity in $\mathrm{Mod}(\mathbb{D}_{2n})$. Suppose $\prod[f_{\sigma(i)}]$ is the identity in $\mathrm{Mod}(\mathbb{D}_{1,n})$. In particular, this means that there is an isotopy h_t from $\prod f_{\sigma(i)}$ to the identity that fixes the marked point in $\mathbb{D}_{1,n}$.

Let h_t be a homotopy at time t from $\mathbb{D}_{n+1}$ to $\mathbb{D}_{n+1}$. Then the homotopy lifting property applies to $h_t \circ q : \mathbb{D}_{2n+1} \to \mathbb{D}_{n+1}$ and fixes the marked puncture in $\mathbb{D}_{n+1}$, which gives us a unique homotopy $\tilde{h}_t : \mathbb{D}_{2n+1} \to \mathbb{D}_{2n+1}$ that fixes the marked puncture in $\mathbb{D}_{2n+1}$. Therefore, we can restrict $\tilde{h}_t$ to go from $\mathbb{D}_{1,2n}$ to $\mathbb{D}_{1,2n}$.

Because $\prod[f_{\sigma(i)}]$ is the identity in $\mathrm{Mod}(\mathbb{D}_{1,n})$, we have that $\tilde{h}_t$ is a homotopy from $\prod \tilde{f}_{\sigma(i)}$ to the identity in $\mathrm{Mod}(\mathbb{D}_{1,2n})$[1]. This means that $[\prod \tilde{f}_{\sigma(i)}]$ and $forget([\prod \tilde{f}_{\sigma(i)}])$ both equal the identity in $\mathrm{Mod}(\mathbb{D}_{2n})$. Therefore, the homomorphism Φ is well defined. □

<u>Part 3</u>:

---

[1]Note that $\tilde{h}_t$ cannot be a homotopy from $\prod \tilde{f}_{\sigma(i)}$ to the involution in $\mathrm{Mod}(\mathbb{D}_{1,2n})$ because the boundary points must be fixed.

Now that we know Φ is a homomorphism, we can prove that it is also injective. But first, we need to define some terminology that is needed for the proof.

Definition 4.4. [MW21] Let $q : S \to X$ be a covering map of surfaces. Map $\tilde{f} : S \to S$ is *fiber preserving* if there exists a map $f : X \to X$ such that the below diagram commutes:

$$
\begin{array}{ccc}
S & \xrightarrow{\tilde{f}} & S \\
{\scriptstyle q}\downarrow & & \downarrow{\scriptstyle q} \\
X & \xrightarrow{f} & X
\end{array}
$$

Definition 4.5. [MW21] Covering map q has the *Birman-Hilden property* if every fiber-preserving homeomorphism that is homotopic to the identity is also homotopic to the identity through fiber-preserving homeomorphisms.

Theorem 4.6. *(Birman-Hilden-Maclachlan–Harvey as cited in [MW21]) Let $q : S \to X$ be a finite-sheeted regular branched covering map where S is a hyperbolic surface. Then q has the Birman–Hilden property.*

Theorem 4.7. $\Phi : Mod(\mathbb{D}_{1,n}) \to Mod(\mathbb{D}_{2n})$ *is injective.*

Proof. Suppose $\Phi(\prod[f_{\sigma(i)}])$ is the homotopy class of the identity $id_{\mathbb{D}_{2n}} : \mathbb{D}_{2n} \to \mathbb{D}_{2n}$. Let $\tilde{f} : \mathbb{D}_{2n} \to \mathbb{D}_{2n}$ be defined such that

$$
\tilde{f}(p) = \begin{cases} (\prod \tilde{f}_{\sigma(i)})(p) & p \in \mathbb{D}_{2n+1} \subseteq \mathbb{D}_{2n} \\ p & p = \mathbb{D}_{2n} \setminus \mathbb{D}_{2n+1} \end{cases} .
$$

By definition, $\Phi(\prod[f_{\sigma(i)}]) = [\tilde{f}] \in \mathrm{Mod}(\mathbb{D}_{2n})$. Because $\Phi(\prod[f_{\sigma(i)}]) = id_{\mathbb{D}_{2n}}$, then $\tilde{f}$ is isotopic to $id_{\mathbb{D}_{2n}}$. Map $\tilde{f}$ is also fiber-preserving because it lifts $\prod f_{\sigma(i)}$.

Because $q_\times : \mathbb{D}_{1,2n} \to \mathbb{D}_{1,n}$ is a two-sheeted regular branched covering map and $\mathbb{D}_{1,2n}$ is a hyperbolic surface, then $q_\times$ has the Birman-Hilden property by Theorem 4.6. This means that $\tilde{f}$ is homotopic to $id_{\mathbb{D}_{2n}}$ through a family of fiber-preserving homeomorphisms $\tilde{h}_t$ that induce a homotopy $h_t : X \to X$ from $\prod f_{\sigma(i)}$ to $id_{\mathbb{D}_{1,n}}$. That is $[\prod f_{\sigma(i)}] = \prod[f_{\sigma(i)}]$ is the identity in $\mathrm{Mod}(\mathbb{D}_{1,n})$ as required. $\square$

Part 4:

We now define the *mixed braid group* and state the relationship between it and the Artin group corresponding to B_n. Then we recall some known isomorphisms between between Artin groups and braid groups and between braid groups and mapping class groups.

Definition 4.8. In [Lam00], Lambropoulou defined the mixed braid group $\mathscr{B}_{g,n}$ to be the subgroup of $\mathscr{B}_{g+n}$ consisting of the set of all braids with g fixed strands and n moving strands. (See also [CL23].) Group $\mathscr{B}_{g,n}$ has two types of generators:

1. g "loop generators" $\alpha_1, ..., \alpha_g$ where α_i is a looping of the 1st moving strand (ms) around the i-th fixed strand (fs):

1$^{\text{st}}$ fs $\quad$ i^{th} fs $\quad$ $(i+1)^{\text{st}}$ fs $\quad$ g^{th} fs $\quad$ 1$^{\text{st}}$ ms $\quad$ n^{th} ms
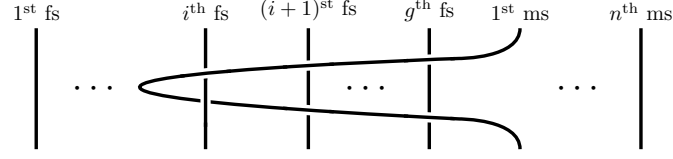
Thus we obtain the following relations between α_i and the standard braid relations θ_1, ..., θ_g where θ_i is the generator between the ith fixed strand and the $(i+1)^{\text{st}}$ fixed strand:

$$\alpha_g = \theta_g^2$$
$$\alpha_{g-1} = \theta_g \theta_{g-1}^2 \theta_g^{-1}$$
$$\alpha_i = \theta_g \theta_{g-1}...\theta_{i+1}\theta_i^2\theta_{i+1}^{-1}...\theta_{g-1}^{-1}\theta_g^{-1} \text{ for } 1 \leq i \leq g.$$

2. $n-1$ elementary crossings σ_1, ..., σ_{n-1} (i.e., moving strands j and $j+1$ interchange positions)

The relations for $\mathscr{B}_{g,n}$ are as follows where the first two are the standard braid relations:

1. $\sigma_i\sigma_j = \sigma_j\sigma_i$, $|i-j| > 1$, $1 \leq i,j \leq n-1$
2. $\sigma_i\sigma_{i+1}\sigma_i = \sigma_{i+1}\sigma_i\sigma_{i+1}$, $1 \leq i \leq n-2$
3. $\alpha_i\sigma_j = \sigma_j\alpha_i$, $1 \leq i \leq g$, $2 \leq j \leq n-1$
4. $\alpha_i\sigma_1\alpha_i\sigma_1 = \sigma_1\alpha_i\sigma_1\alpha_i$, $1 \leq i \leq g$
5. $\alpha_i(\sigma_1\alpha_r\sigma_1^{-1}) = (\sigma_1\alpha_r\sigma_1^{-1})\alpha_i$, $1 \leq r < i \leq g$

In particular, the mixed braid group $\mathscr{B}_{1,n}$ is isomorphic to the Artin group corresponding to B_n. In $\mathscr{B}_{1,n}$, we will call α_1 just α because there is only one fixed strand. Moreover, it is a classic result that $\mathscr{B}_{2n}$ is isomorphic to the Artin group $A(B_{2n-1})$ such that the generators σ_i of $\mathscr{B}_{2n}$ get mapped to the generators t_i of $A(B_{2n-1})$.

Furthermore, we know that the standard braid group $\mathscr{B}_n$ is isomorphic to the mapping class group of the closed disk with n punctures where each generator σ_i of $\mathscr{B}_n$ is mapped to the homotopy class of a homeomorphism of $\mathbb{D}_n$ that corresponds to a half Dehn twist interchanging the ith and $(i+1)^{st}$ punctures (see, for example, Chapter 9 in [FM11]). Thus, $\mathscr{B}_{2n}$ is isomorphic to $\text{Mod}(\mathbb{D}_{2n})$. We can deduce that the mixed braid group $\mathscr{B}_{1,n}$ is also isomorphic to the mapping class group of the closed disk with one marked point and n punctures, $\mathbb{D}_{1,n}$.

Part 5:

We now define the following maps in order to connect $\phi : A(B_n) \to A(A_{2n-1})$ to $\Phi : \text{Mod}(\mathbb{D}_{1,n}) \to \text{Mod}(\mathbb{D}_{2n})$ and show that the two squares in the below diagram commute.

Definition of Maps:

1. Map ι_1 is the standard isomorphism between $A(B_n)$ and $\mathscr{B}_{1,n}$ after reversing the order of the strands in $\mathscr{B}_{1,n}$.
2. Map I_1 is the standard isomorphism between $A(A_{2n-1})$ and $\mathscr{B}_{2n}$.
3. Define ι_2 on generators such that $\iota_2(\alpha) = f_n$ and for $i < n$, $\iota_2(\sigma_{n-i}) = f_i$. Observe that this recovers the usual identification of braids as mapping classes.

$$\begin{array}{ccc}
A(B_n) & \xrightarrow{\ \ \phi\ \ } & A(A_{2n-1}) \\
\iota_1 \Big\downarrow \cong & & \cong \Big\downarrow I_1 \\
\mathscr{B}_{1,n} & \xrightarrow{\ \ \varphi\ \ } & \mathscr{B}_{2n} \\
\iota_2 \Big\downarrow \cong & & \cong \Big\downarrow I_2 \\
\mathrm{Mod}(\mathbb{D}_{1,n}) & \xrightarrow{\ \ \Phi\ \ } & \mathrm{Mod}(\mathbb{D}_{2n})
\end{array}$$

$$\mathrm{Mod}(\mathbb{D}_{1,2n}) \quad \overset{forget}{\nearrow}$$

FIGURE 12. Blueprint of maps

4. Define I_2 on generators corresponding to a half-twist of neighboring strands in the braid group to a half Dehn twist of the corresponding neighboring punctures. Observe that $I_2(\sigma_i' \sigma_{2n-i}') = \tilde{f}_i$ and $I_2(\sigma_n') = \tilde{f}_n$.
5. Define φ on generators such that $\varphi(\alpha) = \sigma_n'$ and for $i < n$, $\varphi(\sigma_{n-i}) = \sigma_{n-(n-i)}' \sigma_{n+(n-i)}' = \sigma_i' \sigma_{2n-i}'$.

With these maps, we see that $I_1\phi = \varphi\iota_1$ and $I_2\varphi = \Phi\iota_2$.

Part 6:

Proof of Proposition 4.2 that $\phi : A(B_n) \to A(A_{2n-1})$ is an injective homomorphism: Because each square diagram in Figure 4 commutes, we have that $I_2 I_1 \phi = \Phi \iota_2 \iota_1$. Because Φ is an injective homomorphism and ι_j and I_j are isomorphisms for $j = 1, 2$, then ϕ is also an injective homomorphism. $\qquad\square$

We finish this section with two remaining statements which will come into use later. The first is implicitly proven in [Hae23, Prop. 6.6]. We will extract its statement and proof here for completeness.

Lemma 4.9. *The vertex $g\hat{t}_i$ is in the image of ψ if and only if $g\hat{t}_i \leq \sigma(g\hat{t}_i)$.*

Proof. First suppose $g\hat{t}_i$ is in the image of ψ. By choosing a different $g \in g\hat{t}_i$, we may assume g is in the image of ϕ. Then

$$\sigma(g\hat{t}_i) = \sigma(g)\hat{t}_{2n-i} = g\hat{t}_{2n-i}.$$

Therefore $g\hat{t}_i \cap \sigma(g\hat{t}_i) \neq \varnothing$ (both sets contain g), so these vertices are either adjacent or equal. In either case, since $i \leq (n+1)/2$, the definition of the partial order implies $g\hat{t}_i \leq \sigma(g\hat{t}_i)$.

Now suppose $g\hat{t}_i \leq \sigma(g\hat{t}_i)$. This implies $g\hat{t}_i \cap \sigma(g\hat{t}_i) = g\hat{t}_i \cap \sigma(g)\hat{t}_{2n-i} \neq \varnothing$. So up to replacing g with some element of $g\hat{t}_i \cap \sigma(g)\hat{t}_{2n-i}$, we may assume $\sigma(g) \in g\hat{t}_{2n-i}$. Choose $h \in \hat{t}_{2n-i}$ such that $\sigma(g) = gh$. Since σ is an involution,

$$g = \sigma(\sigma(g)) = \sigma(gh) = \sigma(g)\sigma(h) = gh\sigma(h).$$

This implies $\sigma(h) = h^{-1} \in \hat{t}_i \cap \hat{t}_{2n-i}$. By [Cha95], h can be factored uniquely as $h = h_1 h_2^{-1}$, with h_1 and h_2 elements of the "positive monoid" $A(A_{2n-1})^+$, such

that the right greatest common divisor of h_1 and h_2 is the identity in the monoid. Moreover, since $h \in \hat{t}_i \cap \hat{t}_{2n-i}$, both h_1 and h_2 are in $\hat{t}_i \cap \hat{t}_{2n-i}$. Then since σ preserves the positive monoid,

$$\sigma(h_1)\sigma(h_2)^{-1} = \sigma(h) = h^{-1} = h_2 h_1^{-1}.$$

But by uniqueness, $h_2 = \sigma(h_1)$, so we can write $h = h_1\sigma(h_1)^{-1}$. Now,

$$\sigma(gh_1) = \sigma(g)\sigma(h_1) = gh\sigma(h_1) = gh_1\sigma(h_1)^{-1}\sigma(h_1) = gh_1,$$

so gh_1 is in the image of ϕ by [Cri00, Thm. 4]. Since $h_1 \in \hat{t}_i$, this means $g\hat{t}_i = gh_1\hat{t}_i$ is in the image of ψ. $\square$

The following is a restatement of [Hua25, Thm. 5.6].

Theorem 4.10. *Suppose v_1, v_2, and v_3 are vertices of $D(A_n)$ of type $\hat{t}_i$ for some $i \geq 3$. Suppose also that each pair of these vertices has a lower bound of type $\hat{t}_i$ or $\hat{t}_{i-1}$. Then there is a vertex v of $D(A_n)$ which is a lower bound of $\{v_1, v_2, v_3\}$ and has type $\hat{t}_i$, $\hat{t}_{i-1}$ or $\hat{t}_{i-2}$.*

5. FILLING LOOPS IN $D(B_3)$

Now we undertake verifying conditions (5) and (6) of Theorem 2.1 for $D(B_3)$.

5.1. **The 4-cycle and 6-cycle.** We begin with the 4-cycle and the 6-cycle, both of which follow easily from our setup.

Lemma 5.1. *Loops in $D(B_3)$ of the type in Figure 2(a) can be filled to subcomplexes of $D(B_3)$ of the type in Figure 3(a).*

Proof. Suppose γ is a(n embedded) loop of this type. The vertices of type $\hat{s}_1$ have a common upper bound, and thus have a least upper bound v By Proposition 4.1. The join v cannot be type $\hat{s}_3$ or $\hat{s}_1$, since this would contradict the assumption that γ is embedded. Thus v is type $\hat{s}_2$. Since v is a least upper bound, both vertices of γ are comparable to v, and in particular there is an edge from v to both of these vertices. Since $D(B_3)$ is flag, this means γ can be filled as claimed. $\square$

Lemma 5.2. *Suppose γ is an embedded closed edge loop in $D(B_3)$ of the form in Figure 2(b). Then γ is contained in a subcomplex of the form in Figure 3(b).*

Proof. The vertices of γ of type $\hat{s}_1$ are pairwise upper bounded by vertices of type $\hat{s}_3$. By Proposition 4.1, this means they have a join, say, v, whose type is $\hat{s}_i$ for some i. This gives a subcomplex of the form
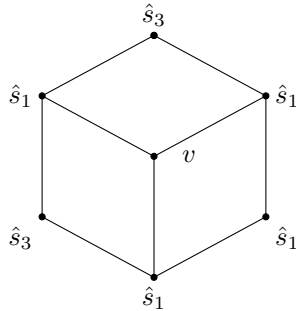
Since γ is embedded, we cannot have $i = 1$. If $i = 2$, then the 4-cycles in this diagram may be filled to obtain a subcomplex of the form in Figure 13 using Lemma 2.11 (the proof of which still applies to $D(B_3)$, even though we have not fully verified conditions (5) and (6)). But in this case, since v is type $\hat{s}_2$, the link of v is complete
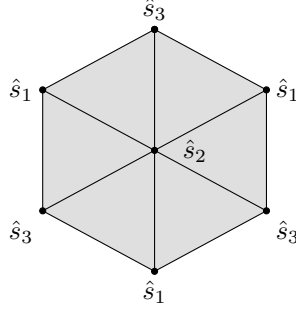

FIGURE 13. A bad filling

bipartite, thus has diameter 4 (under the edge-path metric), implying γ could not be embedded. So we must have $i = 3$, in which case the 4-cycles in the diagram may be filled to obtain a subcomplex of the form in Figure 3(b) using Lemma 5.1. $\square$

5.2. **The 8-cycle.** We next turn our attention to the 8-cycle, which is, in some sense, the first non-trivial case. To do this, we must utilize the material from Section 4 and the geometry of $D(A_5)$.

Lemma 5.3. *If γ is an embedded edge path in $D(B_3)$ of the form in Figure 2(c), then it is contained in a subcomplex of $D(B_3)$ of the form in Figure 3(c).*

Proof. Label the vertices of γ by $v_{i,j}$, where $v_{i,j}$ is type $\hat{s}_i$ and j is assigned as follows:
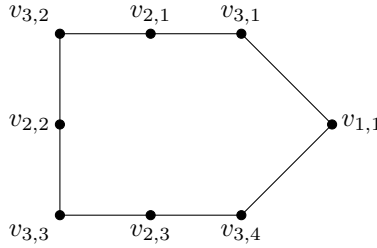

The Hasse diagram of the vertices $V(\gamma)$ of γ under the ordering on the vertices of $D(B_3)$ is as follows:
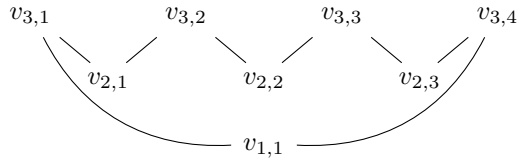

For each i and j, let $u_{i,j} = \psi(v_{i,j})$. Since ψ is an order-preserving injection, the Hasse diagram for the $u_{i,j}$ is identical to that of the $v_{i,j}$. Note that $\sigma(u_{i,j})$ is a

type $\hat{t}_{6-i}$ vertex. Since each $u_{i,j}$ is in the image of ψ, we know $u_{i,j} \leq \sigma(u_{i,j})$. In particular, for each j, since $u_{3,j}$ and $\sigma(u_{3,j})$ are the same type, they must be equal. Since σ is an order-reversing bijection, the Hasse diagram of the $u_{i,j}$ along with their images under σ is as follows:
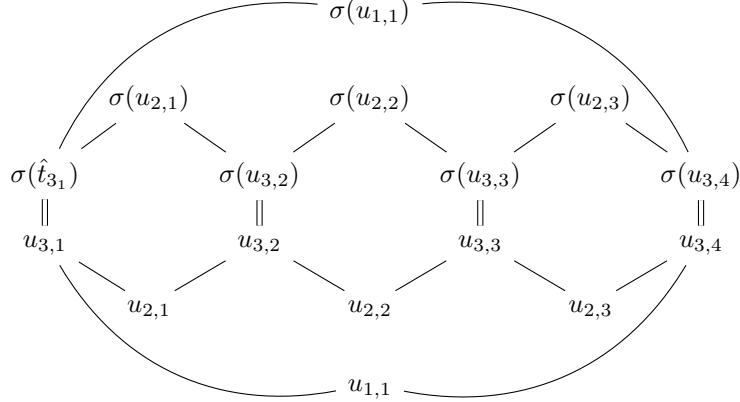

Let w_1 be the join (i.e., the least upper bound) of $u_{2,1}$ and $u_{2,3}$ in $D_0(A_5)$ and let w_2 be the join of $u_{1,1}$ and $u_{2,2}$ in $D_0(A_5)$. Notice that $\sigma(u_{2,2})$ is an upper bound of $u_{2,1}$ and $u_{2,3}$, and $\sigma(u_{2,1})$ is an upper bound of $u_{1,1}$ and $u_{2,2}$. This means w_1 and w_2 are actually contained in $D(A_5)$ (i.e., neither are 0 or 1). Again since σ is an order-reversing injection, $\sigma(w_1)$ is the meet (i.e., greatest lower bound) of $\sigma(u_{2,1})$ and $\sigma(u_{2,3})$, and $\sigma(w_2)$ is the meet of $\sigma(u_{1,1})$ and $\sigma(u_{2,2})$. Adding these points to the above Hasse diagram gives the following:
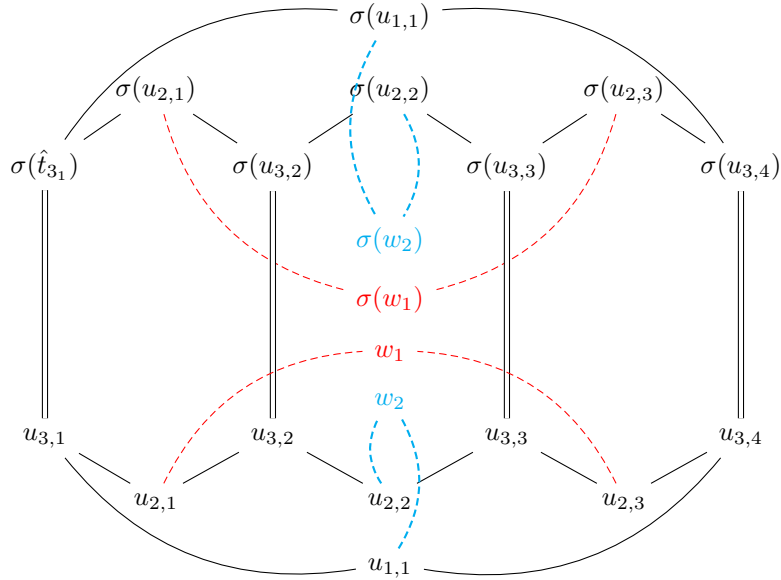
Since we're assuming γ is embedded, both w_1 and w_2 cannot be type $\hat{t}_1$ or type $\hat{t}_2$; otherwise, they would necessarily be equal to one of the $u_{i,j}$ and thus γ would not

have been embedded to start with. This consequently means $\sigma(w_1)$ and $\sigma(w_2)$ are both not type $\hat{t}_5$ or type $\hat{t}_4$.

Now note that $u_{2,1}$ and $u_{2,3}$ are both lower bounds of the set $\{\sigma(u_{1,1}), \sigma(u_{2,2})\}$. Since $\sigma(w_2)$ is the greatest lower bound of this set, $u_{2,1} \le \sigma(w_2)$ and $u_{2,3} \le \sigma(w_2)$. But then $\sigma(w_2)$ is an upper bound for the set $\{u_{2,1}, u_{2,3}\}|$. Since w_1 is the least upper bound of this set, $w_1 \le \sigma(w_2)$. An identical argument shows $w_2 \le \sigma(w_1)$. This means the Hasse diagram is actually as follows:
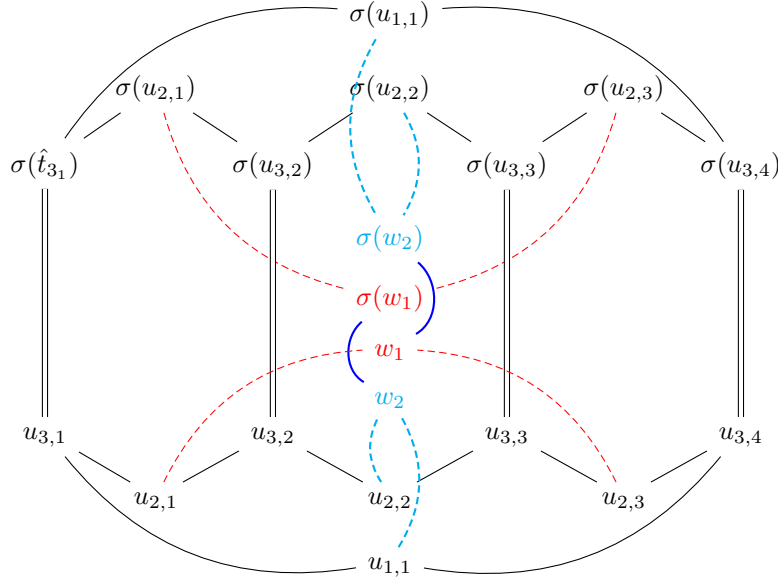

Since w_1 is not type $\hat{t}_1$ or $\hat{t}_2$, and $\sigma(w_2)$ is not type $\hat{t}_4$ or $\hat{t}_5$, it follows that in fact w_1 and $\sigma(w_2)$ are both type $\hat{t}_3$, and so $w_1 = \sigma(w_2)$. Similarly, $w_2 = \sigma(w_1)$ and this vertex is type $\hat{t}_3$.

Consider the vertices w_1, $u_{3,2}$, and $u_{3,3}$. They are type $\hat{t}_3$ vertices which are pairwise lower bounded by vertices of type $\hat{t}_2$. By Theorem 4.10, we can find a vertex z which is a lower bound of all three vertices. Since γ is embedded, z cannot
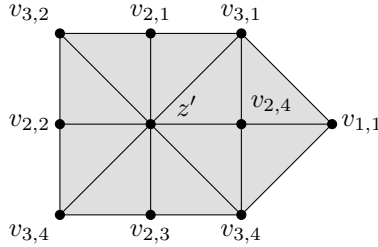
be type $\hat{t}_3$ or $\hat{t}_2$, so it must be type $\hat{t}_1$. Adding z and $\sigma(z)$ to the diagram gives
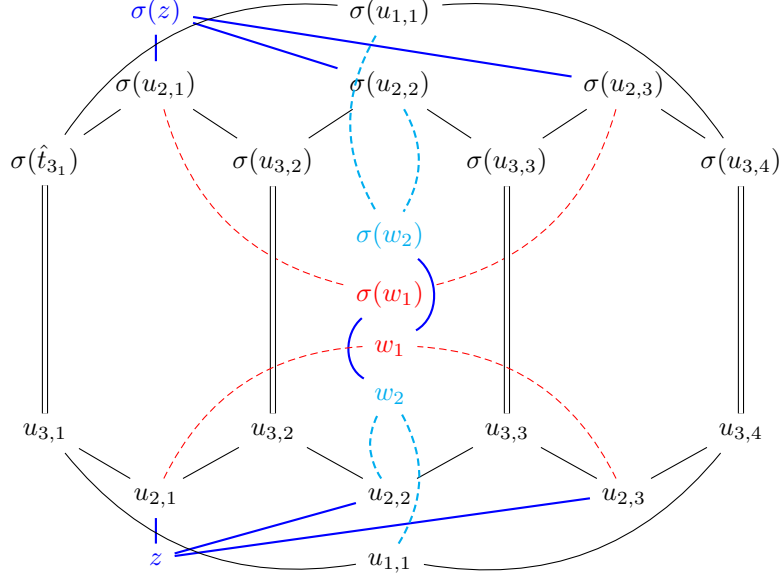
And now we see that $z \leq \sigma(z)$, so by Lemma 4.9, z is in the image of ψ, say $z = \psi(z')$ for some vertex z' of type $\hat{s}_1$. So, we have a subcomplex of $D(B_3)$ of the form
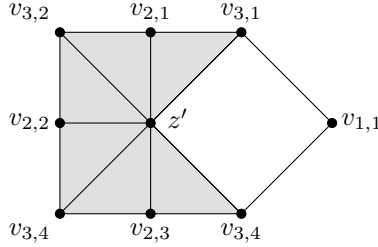
By Lemma 5.1, the 4-cycle made of z, $v_{1,1}$, $v_{3,1}$, and $v_{3,4}$ can be filled with a central vertex $v_{2,4}$ of type $\hat{s}_2$, giving the subcomplex

as claimed. □

5.3. **The 10-cycle.** Last we approach the 10-cycle. In general, a cycle of this length is very difficult to deal with, and progress was only possible with the advent of new methods by Huang [Hua25].

For the rest of this section, let $\tilde{\gamma}$ a cycle of the type in Figure 4. In order to show $\tilde{\gamma}$ is not embedded, our analysis must be broken into two cases, which we describe now. We begin by briefly recalling material defined in [Hua25, §4], rephrasing the definitions in a manner more immediately useful to us (one may readily verify that they are equivalent).

Definition 5.4. Let Γ be a spherical-type Coxeter-Dynkin diagram. Denote by $\rho : D(\Gamma) \to C(\Gamma)$ the quotient map induced by the natural quotient $A(\Gamma) \to W(\Gamma)$. Let $s \in V(\Gamma)$ be a standard generator of $W(\Gamma)$, and let r be any conjugate of s. (In other words, r is a reflection in $W(\Gamma)$.) Let H be the subcomplex of $C(\Gamma)$ fixed (pointwise) by r. Then $C(\Gamma) \setminus H$ has two connected components, permuted isomorphically by r. Choose one of these open components (called a *halfspace*), and let U be the largest (closed) subcomplex of $C(\Gamma)$ contained in this component. We call any lift of U along ρ a *Falk subcomplex of type s in $D(\Gamma)$*.

Remark 5.5. Different choices of lifts of U will give rise to distinct, but isomorphic, choices of Falk subcomplex. For our purposes, the specific choice of Falk subcomplex will be less important than its type. In general, two Falk subcomplexes of the same type will be isomorphic, hence the "type" of a Falk subcomplex is well-defined. To this end, we also emphasize that if two generators t and s are conjugate in $W(\Gamma)$, then a Falk subcomplex of type t is isomorphic to a Falk subcomplex of type s.

We now return to the specific case of B_3. We have the following result regarding Falk subcomplexes in $D(B_3)$:

Proposition 5.6. *Suppose D' is a Falk subcomplex of type s_3 in $D(B_3)$. Then the "orthoscheme metric" on D' is* CAT(0).

Proof. The orthoscheme metric on D' is a piecewise Euclidean metric which, for all 2-simplices, assigns an angle of $\pi/2$ to vertices of type $\hat{s}_2$, and an angle of $\pi/4$ to vertices of both type $\hat{s}_1$ and $\hat{s}_3$. (In other words, every 2-simplex is a Euclidean isosceles right triangle.) After unraveling definitions, [Hua25, Prop. A.1] implies

(1) The link of a vertex of type $\hat{s}_2$ in D' is complete bipartite (in particular, has girth 4), and
(2) The link of a vertex of type $\hat{s}_1$ or $\hat{s}_3$ in D' has girth at least 8.

Hence this metric is CAT(0). $\qquad\qquad\square$

Since these subcomplexes carry a nice CAT(0) metric, we will call any Falk subcomplex of type $\hat{s}_3$ a *good Falk subcomplex*. Our first case in the analysis of 10-cycles is the following.

Lemma 5.7. *If $\tilde{\gamma}$ is contained in a good Falk subcomplex, then it is not embedded.*

Proof. Suppose D' is a good Falk subcomplex containing $\tilde{\gamma}$. If $\tilde{\gamma}$ is locally geodesic under the orthoscheme metric, then since this metric is CAT(0), we would have that $\tilde{\gamma}$ is a global geodesic, and hence not closed. So there must be some point at which $\tilde{\gamma}$ is not locally geodesic in the orthoscheme metric. It is clear that interiors of edges are always geodesic. It follows from the fact that the link of a $\hat{s}_2$ vertex is complete bipartite that $\tilde{\gamma}$ is always locally geodesic at vertices of type $\hat{s}_2$. Hence there must be some vertex v of type $\hat{s}_3$ at which γ fails to be locally geodesic. Let $v_{-2}, v_{-1}, v_0, v_1, v_2$ be a sequence of adjacent (distinct) vertices with $v_0 = v$, and let δ denote the subpath of $\tilde{\gamma}$ from v_{-2} to v_2 passing through v_0. In the orthoscheme

metric on D', the link of v is a bipartite graph with edge lengths all $\pi/4$. Hence the only way for $\tilde{\gamma}$ to fail to be locally geodesic at v is for there to exist a vertex w of type $\hat{s}_1$ adjacent to each of v_{-1}, v_0, and v_1 (see Figure 14). Since v_{-1} and v_1 are
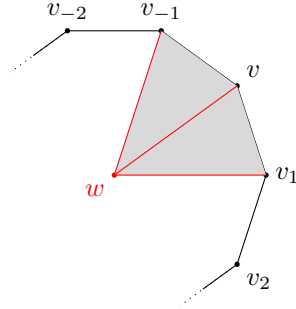

FIGURE 14. Adding a vertex of type $\hat{s}_1$

type $\hat{s}_2$, their links are also complete bipartite, so w must also be adjacent to v_{-2} and v_2 (see Figure 15). Let δ' denote the concatenation of the segments between
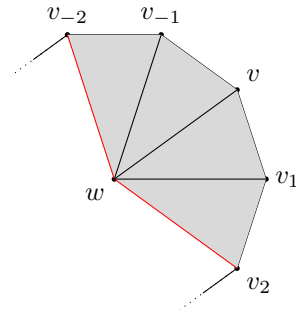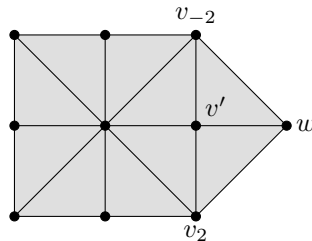

FIGURE 15. Connecting the new vertex to the adjacent type $\hat{s}_2$ vertices

v_{-2} and w, and between w and v_2. Let $\tilde{\gamma}'$ be the cycle obtained from $\tilde{\gamma}$ by replacing δ with δ'. Then $\tilde{\gamma}'$ is an 8-cycle in $D(B_3)$ of the form seen in Figure 2(c), thus can be filled to the following subcomplex:

Let v' be the new type $\hat{s}_2$ vertex adjacent to each of v_{-2}, w, and v_2. The vertices v', v_{-2}, v_{-1}, v, v_1, and v_2 give rise to a 6-cycle in the link of w. However, w is type $\hat{s}_1$, and the link of such a vertex has girth 8. Hence this 6-cycle cannot be

embedded. Regardless of which vertices are identified in this cycle, it results in $\tilde{\gamma}$ not being embedded in $D(B_3)$, as well.

$\square$

It remains to consider those 10-cycles which do not remain in a good Falk subcomplex. In order to complete this argument, we must utilize the "pure Salvetti complex" of $A(\Gamma)$. As to not get bogged down in details, we will leave the full definition to [Hua25, §4.2]; however, here, we adopt the notation $\widehat{\Sigma}(\Gamma)$ (rather than $\widehat{\Sigma}_{\mathcal{A}}$) for consistency. The following are facts regarding $\widehat{\Sigma}(\Gamma)$ which will be relevant for us:

(1) $\pi_1(\widehat{\Sigma}(\Gamma))$ is the kernel of the quotient homomorphism $A(\Gamma) \to W(\Gamma)$ (called the *pure Artin group*, denoted $PA(\Gamma)$)
(2) There is a projection map $p = p_\Gamma : \widehat{\Sigma}(\Gamma) \to \Sigma(\Gamma)$ which is a bijection of vertex sets.
(3) If F is a face of $\Sigma(\Gamma)$ and $\widehat{F} = p^{-1}(F)$, then there is a retraction $\mathrm{Proj}_{\widehat{F}} : \widehat{\Sigma}(\Gamma) \to \widehat{F}$ which restricts to the "closest point" projection on the 1-skeleton (under the path metric). In particular, the inclusion $\widehat{F} \hookrightarrow \widehat{\Sigma}(\Gamma)$ is π_1-injective.

We can give a more explicit (and standard) description of (1). Recall that the 1-skeleton of $\Sigma(\Gamma)$ is the (unoriented) Cayley graph of $W(\Gamma)$ with respect to the standard generating set, so we may label edges by generators. We can then pull back this labeling along the projection $p : \widehat{\Sigma}(\Gamma) \to \Sigma(\Gamma)$ so that all edges of $\widehat{\Sigma}(\Gamma)$ are labeled by a generator. For each edge e of $\Sigma(\Gamma)$, $p^{-1}(e)$ consists of exactly two edges (and two vertices) of $\widehat{\Sigma}(\Gamma)$. We assign these edges "opposite" orientations. Now we fix a base point $x \in V(\widehat{\Sigma}(\Gamma))$ and choose a word $w = s_1^{k_1} \dots s_n^{k_n}$ in $PA(\Gamma)$. If $k_1 > 0$, then we loop around the edges adjacent to x labeled s_1 in the positive orientation k_1 times. If $k_1 < 0$, then we do the same but in the negative orientation. The end of this path may or may not be x, but regardless, we repeat this with s_2, and so on. This procedure will give a closed loop in $\widehat{\Sigma}(\Gamma)$ representing w in $\pi_1(\widehat{\Sigma}(\Gamma))$. In particular, if w is trivial, then this loop will be nullhomotopic.

We can now return to our analysis of $\tilde{\gamma}$. Our goal is to construct a word in $PA(\Gamma)$ using $\tilde{\gamma}$, then pass to a loop in $\widehat{\Sigma}(B_3)$ using the above construction in order to determine more information about $\tilde{\gamma}$. Since the vertices of type $\hat{s}_2$ are complete bipartite, we can fill $\tilde{\gamma}$ into the following diagram:
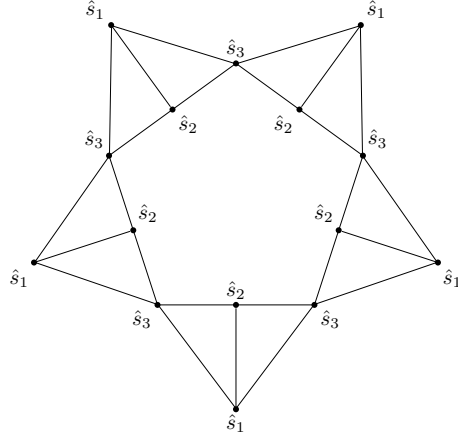
Just as an edge is labeled by the intersection of its vertices, we can label a 2-simplex by the intersection of its vertices. This will be a coset of the trivial subgroup, i.e., a single group element, so we may as well label a 2-simplex solely by this element.
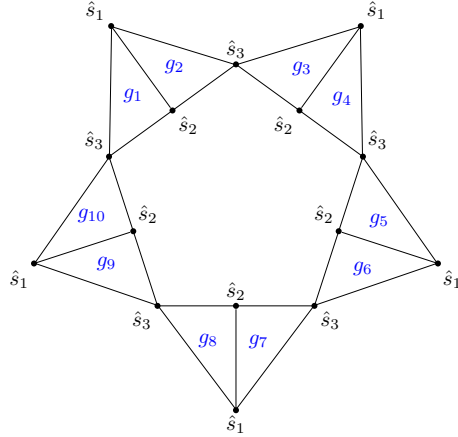
Suppose we have adjacent 2-simplices $\sigma_1 = \{h_1\}$ and $\sigma_2 = \{h_2\}$ with α the edge or vertex at which they meet. Then there is an element $a \in \alpha$ (recall α is a coset of a standard parabolic subgroup) such that $\sigma_1 = a\sigma_2$, or in the group, $h_1 = ah_2$. Returning to the diagram and utilizing this observation, we see there is some $a_1 \in A(s_3)$ such that $g_2 = a_1 g_1$. Of course, since $a_1 \in A(s_3)$, we may write $a_1 = s_3^{n_1}$ for some $n_1 \in \mathbb{Z}$. Similarly, there is some $a_2 \in A(\hat{s}_3)$ such that $g_3 = a_2 g_2$. Repeating, we have $g_{2k} = a_{2k} g_{2k-1}$ where $a_{2k} = s_3^{n_{2k}}$, and $g_{2k+1} = a_{2k+1} g_{2k}$ where $a_{2k+1} \in A(\hat{s}_3)$. But importantly, since this is a cycle, we also have that $g_1 = a_{10} g_{10}$ where $a_{10} \in A(\hat{s}_3)$. Combining these equations gives us the trivial word

$$w = a_1 a_2 \ldots a_{10}.$$

In particular, $w \in PA(\Gamma)$, so there is a loop γ representing w in $\widehat{\Sigma}(\Gamma)$ as constructed previously (and since w is trivial, γ is nullhomotopic).

Definition 5.8. Let E be an edge of $\Sigma(B_3)$ labeled s, for $s = s_1, s_2$, or s_3. We call $\hat{E} := p^{-1}(E)$ an *s loop*. Let F be a 2-cell of $\Sigma(B_3)$. Then F is either a square,
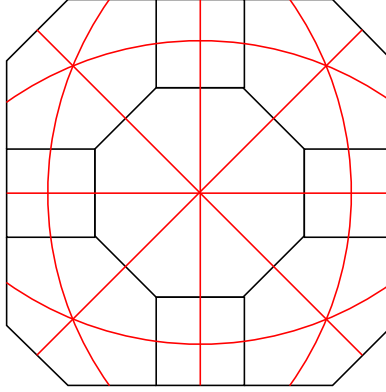
FIGURE 16. A portion of $\Sigma(B_3)$ corresponding to the good Falk subcomplex, with the Coxeter complex cell structure overlaid in red.

hexagon, or octagon, and we will call $\hat{F} := p^{-1}(F)$ a *square, hexagon, or octagon* of $\widehat{\Sigma}(B_3)$, respectively. We will call $\hat{E}$ and $\hat{F}$ *special subcomplexes* of $\widehat{\Sigma}(B_3)$.

Suppose $\hat{F}$ and $\hat{G}$ are special subcomplexes of $\widehat{\Sigma}(B_3)$. We will say that γ *leaves $\hat{F}$ and enters $\hat{G}$ at time t* if for all small $\varepsilon > 0$, we have that

(1) $\gamma(t) \in \hat{F} \cap \hat{G}$,
(2) $\gamma(t + \varepsilon) \in \hat{G}$, and
(3) $\gamma(t + \varepsilon) \notin \hat{F}$.

A subword $a_i \in A(\hat{s}_3)$ of w gives rise to a time t where γ leaves a square and enters a hexagon. A subword $a_i \in A(s_3)$ gives rise to a time t where γ leaves a hexagon and enters a square; more specifically, it enters an s_3 loop. Notice that this means γ must enter hexagons 5 times and must enter squares 5 times.

The next lemma follows immediately from unraveling the full definitions found in [Hua25].

Lemma 5.9. *Let U denote the subcomplex of $\Sigma(B_3)$ seen in Figure 16, and let $\widehat{U} = p^{-1}(U) \subseteq \widehat{\Sigma}(B_3)$. Then $\tilde{\gamma}$ stays in a good Falk subcomplex if and only if γ stays in a subcomplex of $\widehat{\Sigma}(B_3)$ isomorphic to $\widehat{U}$.*

From this, we can show that 10-cycles leaving a good Falk subcomplex must have a certain form in $\widehat{\Sigma}(B_3)$.

Lemma 5.10. *If $\tilde{\gamma}$ is not contained in a good Falk complex, then there is (at least) one square $S \subseteq \Sigma(B_3)$ such that*

(1) *γ enters $\hat{S}$ exactly one time, and*
(2) *If H is the hyperplane of $\Sigma(B_3)$ dual to the s_3 edges of S, and $\hat{F} \neq \hat{S}$ is a hexagon or square which γ enters, then $p(\hat{F}) \cap H = \varnothing$.*

Proof. We can group the possibilities for γ based on the number of distinct hexagons it enters. Throughout, let U be a subcomplex of $\Sigma(B_3)$ of the form shown in Figure 16, and let $\hat{U} = p^{-1}(U)$.
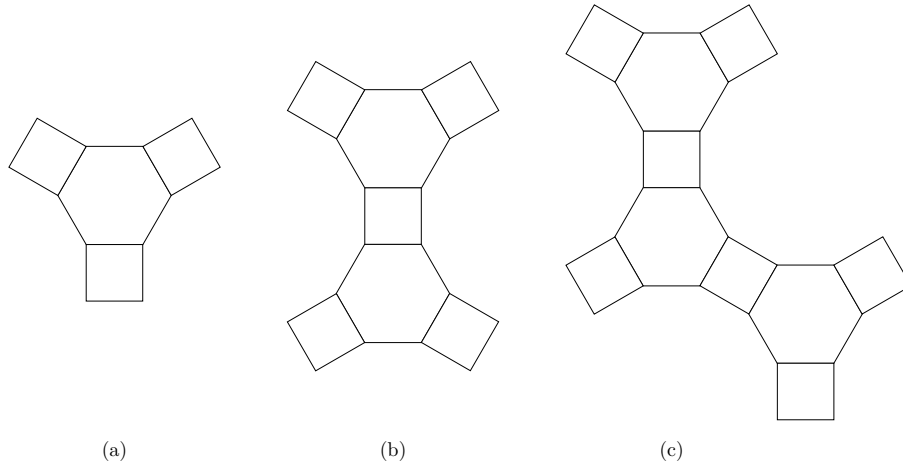
FIGURE 17. Various subcomplexes of $\Sigma(B_3)$

Suppose γ enters exactly one hexagon (possibly multiple times). Then γ remains in a subcomplex of $\widehat{\Sigma}(B_3)$ of the form $p^{-1}(K)$, where K has the shape seen in Figure 17(a). If it enters one or two of the adjacent squares, then it is contained in some $\hat{U}$, and so $\tilde{\gamma}$ is contained in a good Falk complex. If instead it enters three squares, then it must enter one of them exactly once, and the hyperplane dual to this square's s_3 edges satisfies the conclusion of the Lemma.

Suppose γ enters exactly two hexagons. Then γ remains in a subcomplex of $\widehat{\Sigma}(B_3)$ of the form $p^{-1}(K)$, where K has the shape seen in Figure 17(b). Note that there is exactly one square between these hexagons, and γ must enter it an even number of times in order to be a closed loop. Thus γ may enter exactly one, two, or, three other squares. If γ enters one other square, or two other squares in the configuration seen in Figure 18(a), then it is contained in some $\hat{U}$, so $\tilde{\gamma}$ is contained in a good Falk subcomplex. Otherwise, there must be some square which it intersects exactly once, and the hyperplane dual to this square's s_3 edges satisfies the conclusion of the Lemma.

Suppose γ enters exactly three hexagons. Then γ remains in a subcomplex of $\widehat{\Sigma}(B_3)$ of the form $p^{-1}(K)$, where K has the shape seen in Figure 17(c). In order to enter all three hexagons, it must enter the squares between them at least 4 times. Therefore there is at most one other square it can enter. If it stays within a subcomplex of the form seen in Figure 18(b), then it is contained in some $\hat{U}$, so $\tilde{\gamma}$ is contained in a good Falk subcomplex. If not, then the s_3 edges of any of the three remaining squares satisfy the conclusions of the Lemma.

Suppose γ enters exactly four hexagons. Then since γ must enter the squares between each hexagon at least once, it must remain in a subcomplex of $\widehat{\Sigma}(B_3)$ of the form $p^{-1}(K)$, where K has the shape seen in Figure 19. If γ does not enter the extra top-right square, then it is contained in some $\hat{U}$, so $\tilde{\gamma}$ is contained in a good Falk subcomplex. If it does enter this square, then it can do so only once, and the s_3 edges of this square satisfy the conclusions of the Lemma.
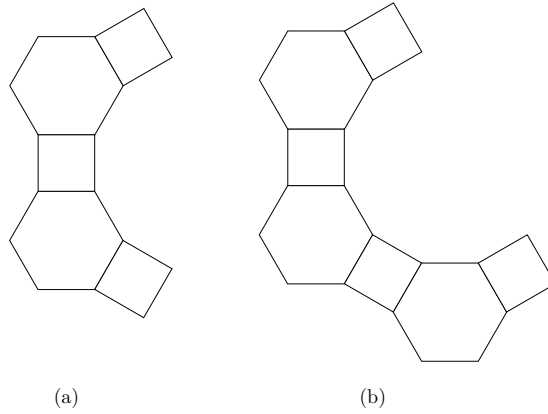
(a)   (b)
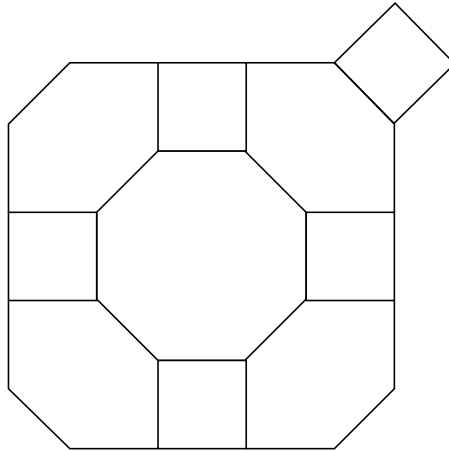
FIGURE 18. Good configurations

FIGURE 19. The 4-hexagon subcomplex

Note that γ may not enter more than 4 distinct hexagons, as this would require it to enter squares more than 5 times. Thus we have exhausted all possibilities for γ.   □

Now we may complete the proof of the remaining case. Our argument will follow a similar structure to many of the core ideas of [Hua25].

Lemma 5.11. *If $\tilde{\gamma}$ is not contained in a good Falk subcomplex, then it is not embedded.*

Proof. Consider the square S and hyperplane H guaranteed by 5.10. Our prior remarks imply that γ only enters a single s_3 loop $\hat{E}$ of $\hat{S}$, say at time t_0. Consider the projection $\mathrm{Proj}_{\hat{E}}$. If $\hat{F} \neq \hat{S}$ is a square or hexagon which γ enters, then since $p(\hat{F}) \cap H = \varnothing$ and H is the hyperplane dual to E, we must have that $\mathrm{Proj}_{\hat{E}}(\hat{F})$ is a vertex $\hat{v}_{\hat{F}}$ of $\hat{E}$. But since γ is closed and enters $\hat{E}$ exactly once, every such

hexagon or square must lay on the same side of H, so there is a vertex $\hat{v}$ of $\hat{E}$ such that $\hat{v} = \hat{v}_{\hat{F}}$ for all such $\hat{F}$.

Since $\mathrm{Proj}_{\hat{E}}$ is a topological retraction, it induces a group-theoretic retraction

$$(\mathrm{Proj}_{\hat{E}})_* : \pi_1(\widehat{\Sigma}(B_3)) \cong PA(B_3) \to \pi_1(\hat{E}) \cong PA(s_3).$$

The group-theoretic translation of the previous paragraph is simply

$$(\mathrm{Proj}_{\hat{E}})_*(w) = a_i,$$

where $a_i \in A(s_3)$ is the subword representing γ entering $\hat{S}$ at time t_0. But w is trivial (or, topologically, γ is nullhomotopic), and this is a retract, so this implies a_i is also trivial (or, topologically, $\mathrm{Proj}_{\hat{E}}(\gamma)$ is still nullhomotopic). Then $g_{i+1} = a_i g_i = g_i$, so $\tilde{\gamma}$ is not embedded. $\square$

This concludes the verification that all closed loops can be filled, so we may finally conclude

Theorem 5.12. *The (piecewise spherical) Moussong metric on the spherical Deligne complex of type B_3 is* CAT(1).

Proof. We will show that $D(B_3)$ satisfies the hypotheses of Theorem 2.1. First, it follows quickly from [CD95] that $D(B_3)$ satisfies conditions (1), (2), (3), and (4). Lemmas 5.1, 5.2, and 5.3 imply condition (5) is satisfied. Last, Lemmas 5.7 and 5.11 show that condition (6) is satisfied. $\square$

This quickly implies the following.

Theorem 5.13. *Suppose $A(\Gamma)$ is a 3-dimensional Artin group and Γ contains no subdiagram of type H_3. Then the (piecewise Euclidean) Moussong metric on the Deligne complex for $A(\Gamma)$ is* CAT(0) *and, in particular, $A(\Gamma)$ satisfies the $K(\pi, 1)$ conjecture.*

Proof. This follows from applying Proposition 3.1, noticing that, by the classification of spherical Coxeter-Dynkin diagrams, the (maximal) connected diagrams Λ in $\mathcal{S}_\Gamma^f$ are either dihedral, type A_3, or type B_3. In the first case, the Moussong metric on $D(\Lambda)$ is CAT(1) by [CD95]. In the second case, the Moussong metric on $D(\Lambda)$ is CAT(1) by [Cha04]. And, in the last case, the Moussong metric on $D(\Lambda)$ is CAT(1) by Theorem 2.9. $\square$

References

[BH13]   Martin R Bridson and André Haefliger. *Metric spaces of non-positive curvature*, volume 319. Springer Science & Business Media, 2013.

[Bow95] Brian H Bowditch. Notes on locally CAT(1) spaces. *Geometric group theory (Columbus, OH, 1992)*, 3:1–48, 1995.

[CD95]   Ruth Charney and Michael W Davis. The $K(\pi,1)$-problem for hyperplane complements associated to infinite reflection groups. *Journal of the American Mathematical Society*, 8(3):597–627, 1995.

[Cha95] Ruth Charney. Geodesic automation and growth functions for artin groups of finite type. *Mathematische Annalen*, 301(1):307–324, 1995.

[Cha04] Ruth Charney. The Deligne complex for the four-strand braid group. *Transactions of the American Mathematical Society*, 356(10):3881–3897, 2004.

[CL23]   Paolo Cavicchioli and Sofia Lambropoulou. The mixed hilden braid group and the plat equivalence in handlebodies. *arXiv preprint arXiv:2312.10781*, 2023.

[Cri97] John Crisp. *Injective maps between Artin groups*. University of Sydney. School of Mathematics and Statistics, 1997.

[Cri00]   John Crisp. Symmetrical subgroups of artin groups. *Advances in Mathematics*, 152(1):159–177, 2000.

[EM02]   Murray Elder and Jon McCammond. Curvature testing in 3-dimensional metric polyhedral complexes. *Experimental Mathematics*, 11(1):143–158, 2002.

[FM11]   Benson Farb and Dan Margalit. *A primer on mapping class groups*, volume 41. Princeton University Press, 2011.

[Gol25]   Katherine M Goldman. CAT(0) and cubulated Shephard groups. *Journal of the London Mathematical Society*, 111(1):e70050, 2025.

[Hae23]   Thomas Haettel. Lattices, injective metrics and the $K(\pi, 1)$ conjecture. *arXiv preprint arXiv:2109.07891v5*, 2023.

[Hua24]   Jingyin Huang. Labeled four cycles and the $K(\pi, 1)$-conjecture for Artin groups. *Inventiones mathematicae*, 238(3):905–994, 2024.

[Hua25]   Jingyin Huang. Cycles in spherical Deligne complexes and application to $K(\pi, 1)$-conjecture for Artin groups. *arXiv preprint arXiv:2405.12068*, 2025.

[Lam00]   Sofia Lambropoulou. Braid structures in knot complements, handlebodies and 3–manifolds. In *Knots In Hellas' 98*, pages 274–289. World Scientific, 2000.

[MW21]   Dan Margalit and Rebecca R Winarski. Braid groups and mapping class groups: The birman–hilden theory. *Bulletin of the London Mathematical Society*, 53(3):643–659, 2021.

[PS21]   Giovanni Paolini and Mario Salvetti. Proof of the $K(\pi, 1)$ conjecture for affine Artin groups. *Inventiones mathematicae*, 224(2):487–572, 2021.

[vdL83]   H. van der Lek. *The homotopy type of complex hyperplane complements*. PhD thesis, Katholieke Universiteit te Nijmegen, 1983.